Supplement of Atmos. Chem. Phys., 21, 12867–12894, 2021
https://doi.org/10.5194/acp-21-12867-2021-supplement

Atmospheric Chemistry and Physics
Open Access
EGU

Supplement of

Technical note: Evaluation of profile retrievals of aerosols and trace gases for MAX-DOAS measurements under different aerosol scenarios based on radiative transfer simulations

Xin Tian et al.

Correspondence to: Pinhua Xie (phxie@aiofm.ac.cn) and Yang Wang (y.wang@mpic.de)

Supplement

(a) Exponential

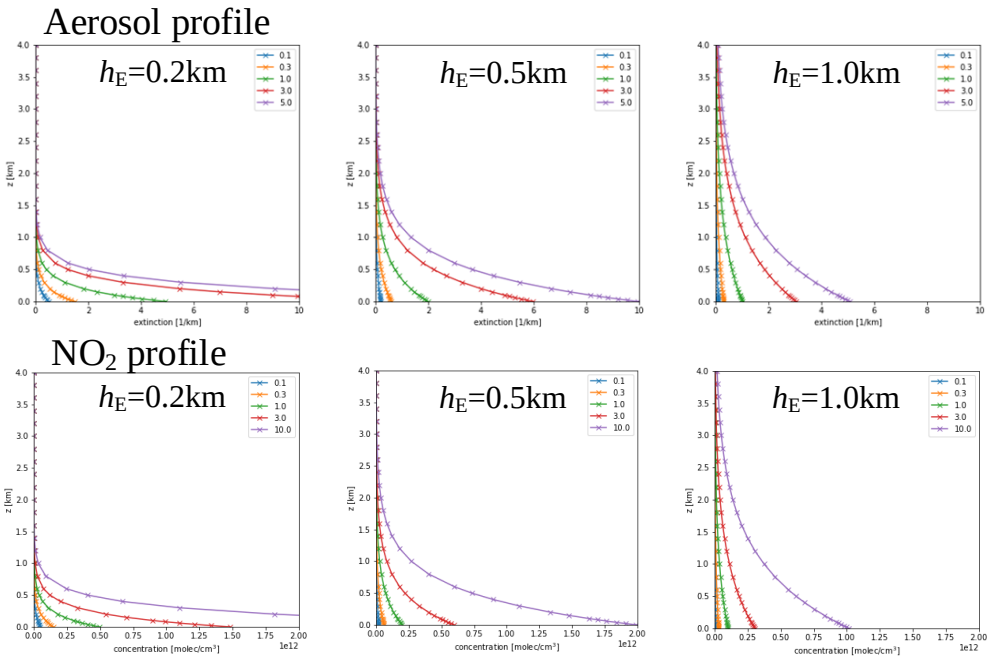

(b) Boltzmann

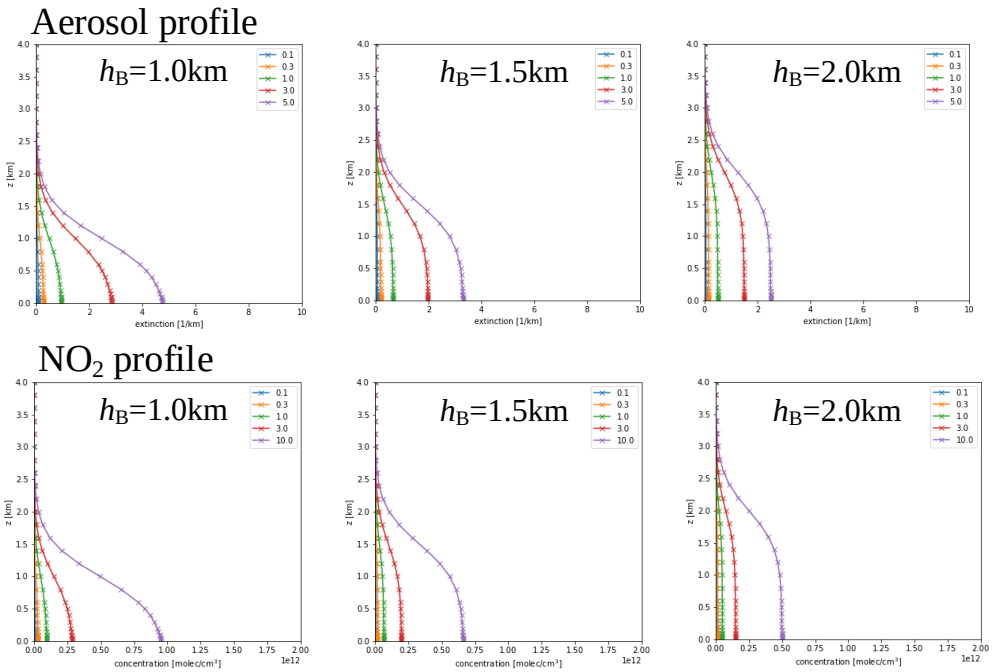

(c) Gaussian

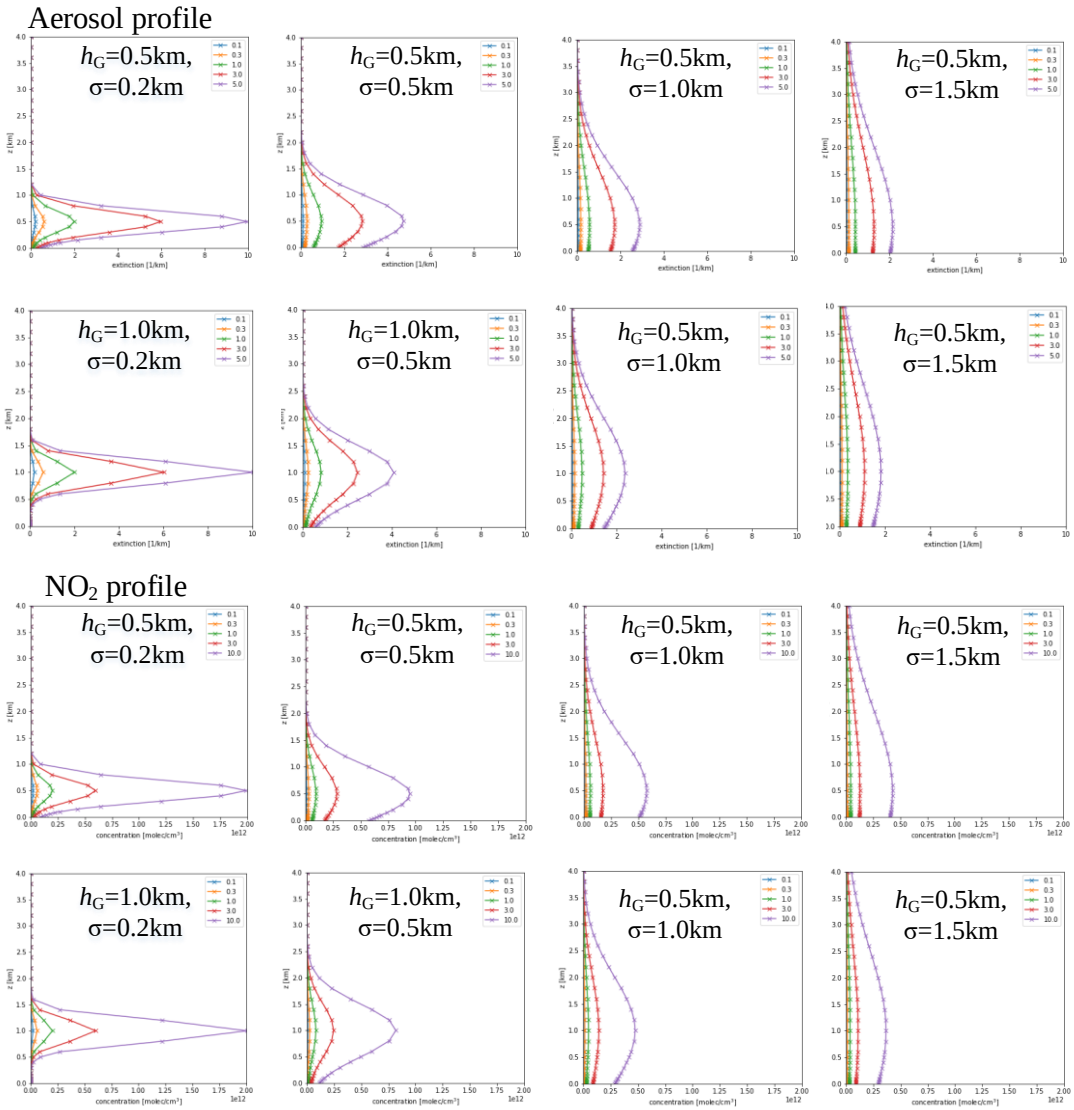

Figure S1. Overview on the tested profile shapes using the 3 different parameterisations with different height parameters: (a) exponential shape, (b)Boltzmann shape, and (c) Gaussian shape. The colors refer to the AOD/VCD values shown at the top right. The VCD in the figure legend is given in 10^{16} molec. /cm^2.

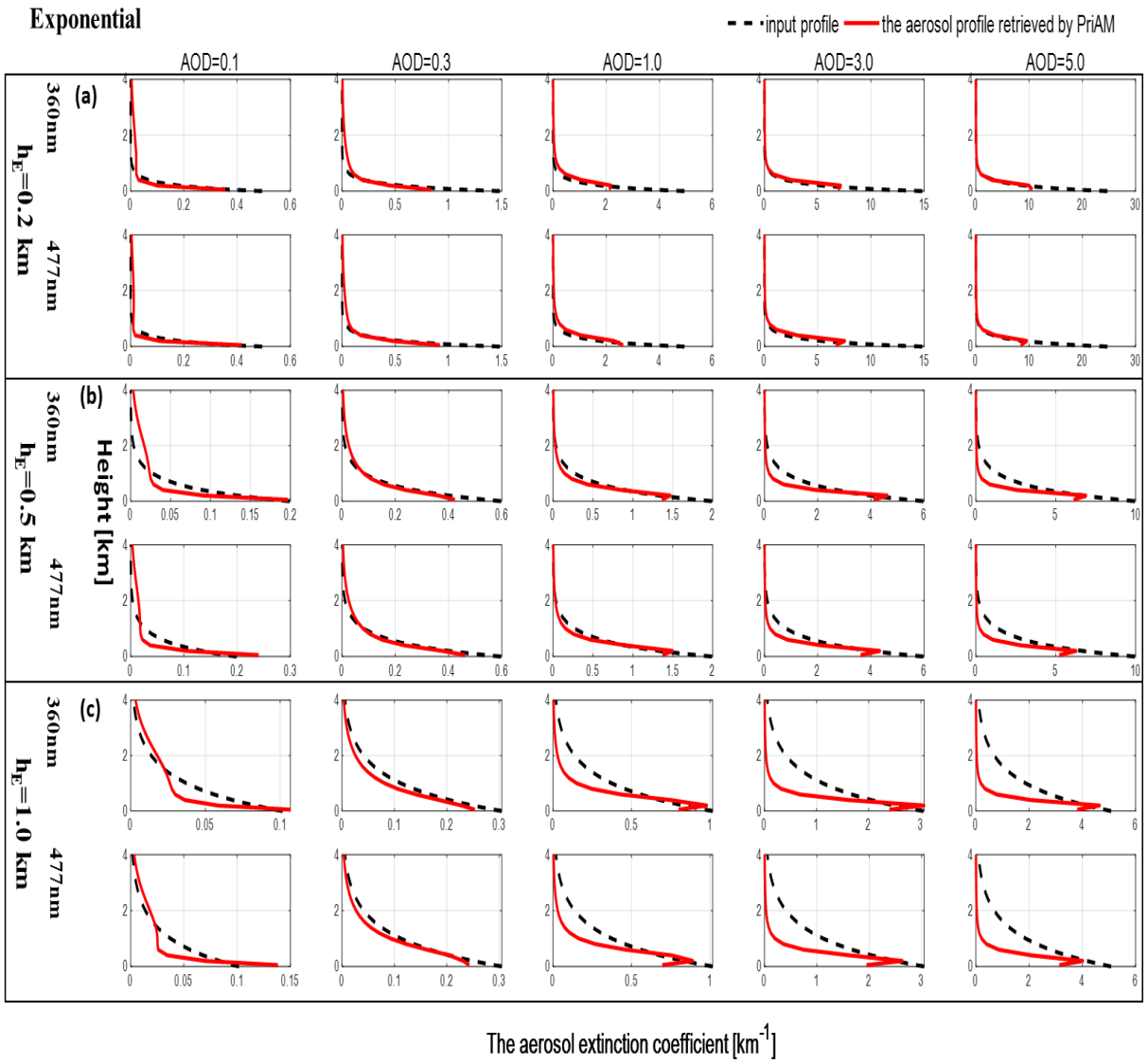

Figure S2. Comparison of aerosol profiles retrieved by PriAM for 360nm (first line) and 477nm (Second line) with the corresponding input aerosol profiles for exponential shape with scale heights of (a) h_E=0.2km, (b) h_E=0.5km, and (c) h_E=1.0km

The black and red curves indicate the input and retrieved aerosol profiles by PriAM, respectively.

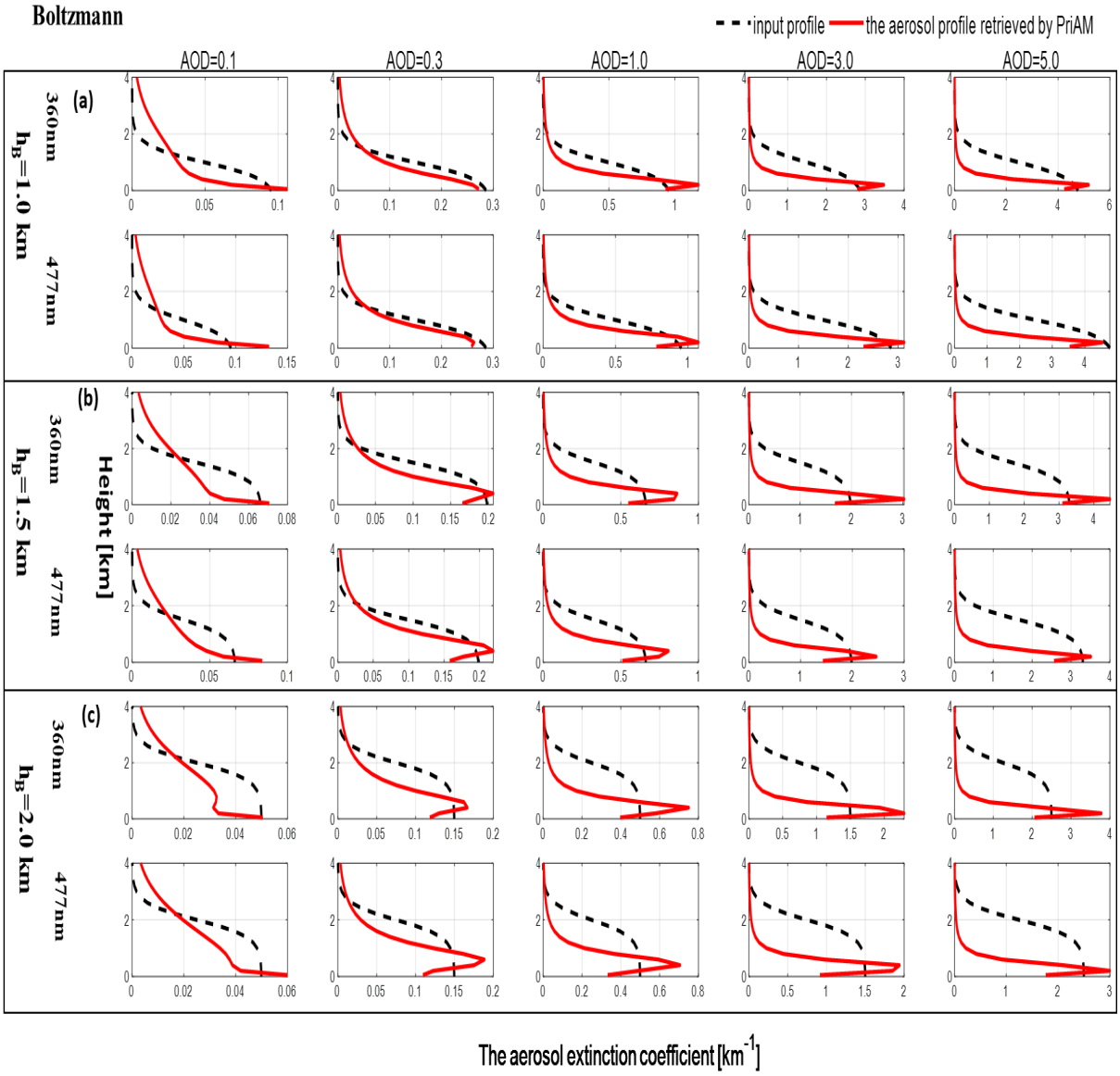

Figure S3. Comparison of aerosol profiles retrieved by PriAM for 360nm (first line) and 477nm (Second line) with the corresponding input aerosol profiles for Boltzmann shape with height parameter (a) h_B=1.0km, (b) h_B=1.5km, and (c) h_B=2.0km

The black and red curves indicate the input and retrieved aerosol profiles by PriAM, respectively.

(I) Gaussian @ h_G= 0.5 km

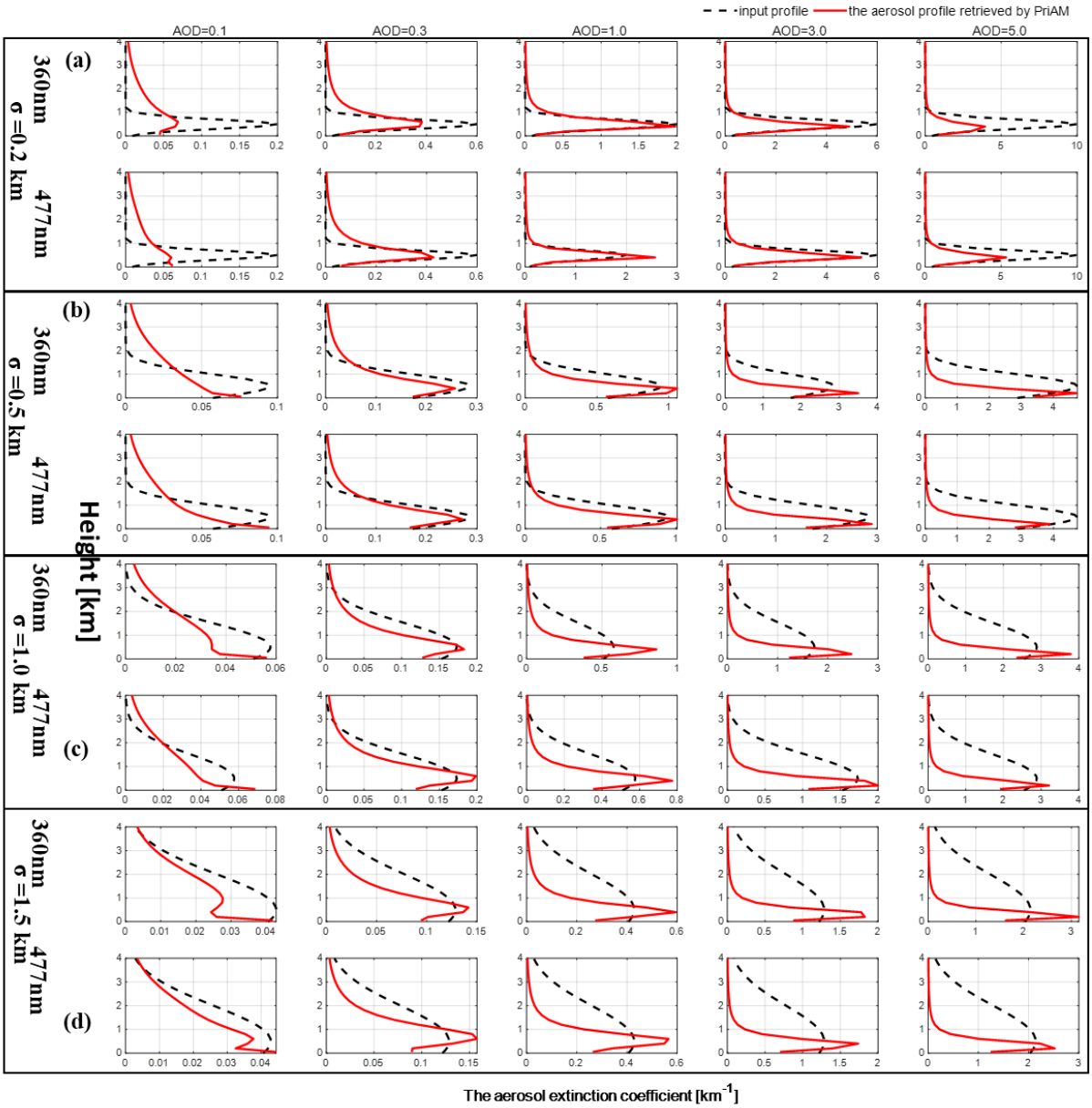

(II) Gaussian @ h_G= 1.0 km

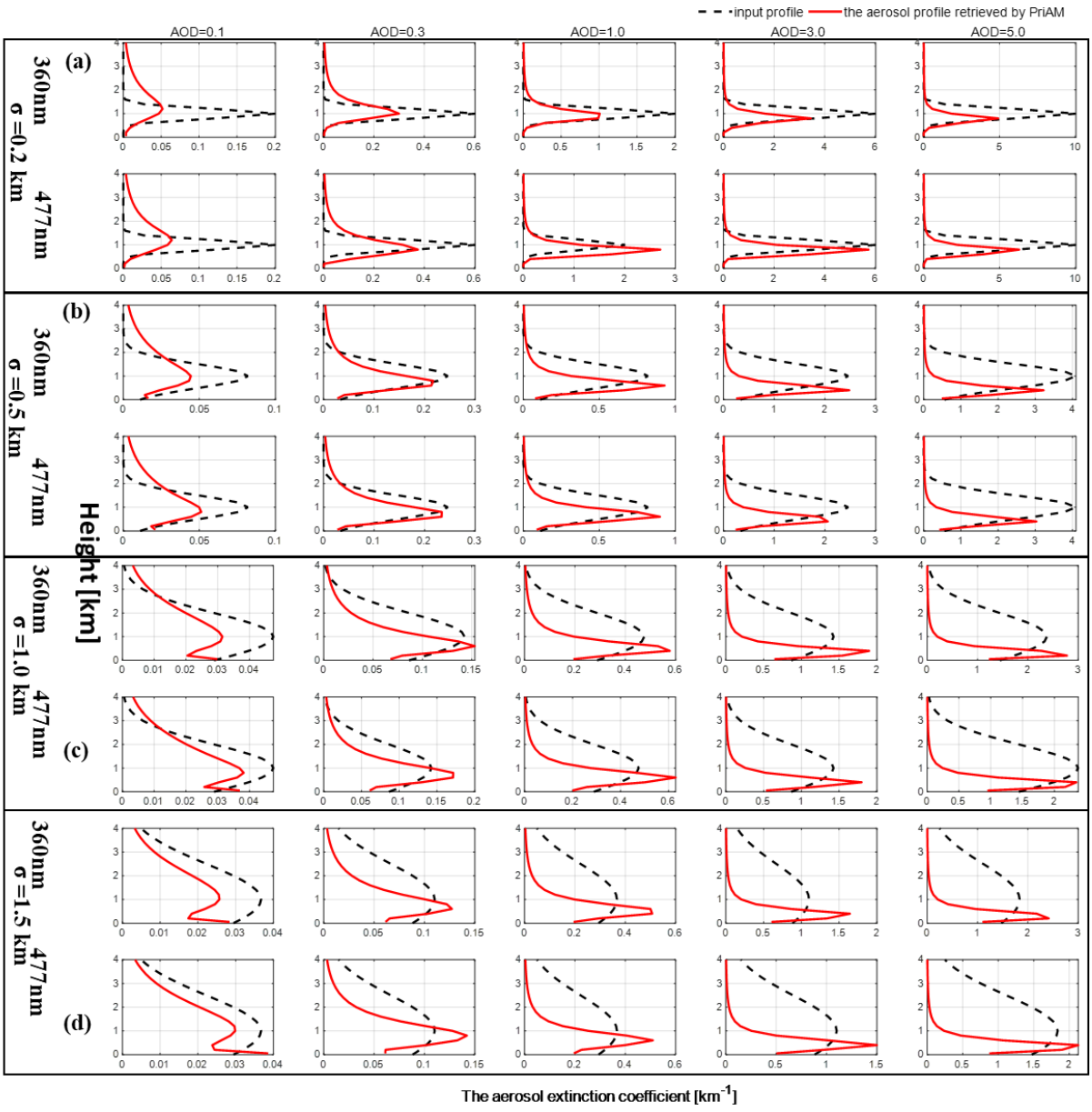

Figure S4. Comparison of aerosol profiles retrieved by PriAM for 360nm (first line) and 477nm (Second line) with the corresponding input aerosol profiles for Gaussian shape with different peak heights z_{peak} (I) h_G=0.5km and (II) h_G=1.0km of full width at half maximum (FWHM) σ (a) σ=0.2km, (b) σ=0.5km, (c) σ =1.0km, and (d) σ =1.5km.

The black and red curves indicate the input and retrieved aerosol profiles by PriAM, respectively.

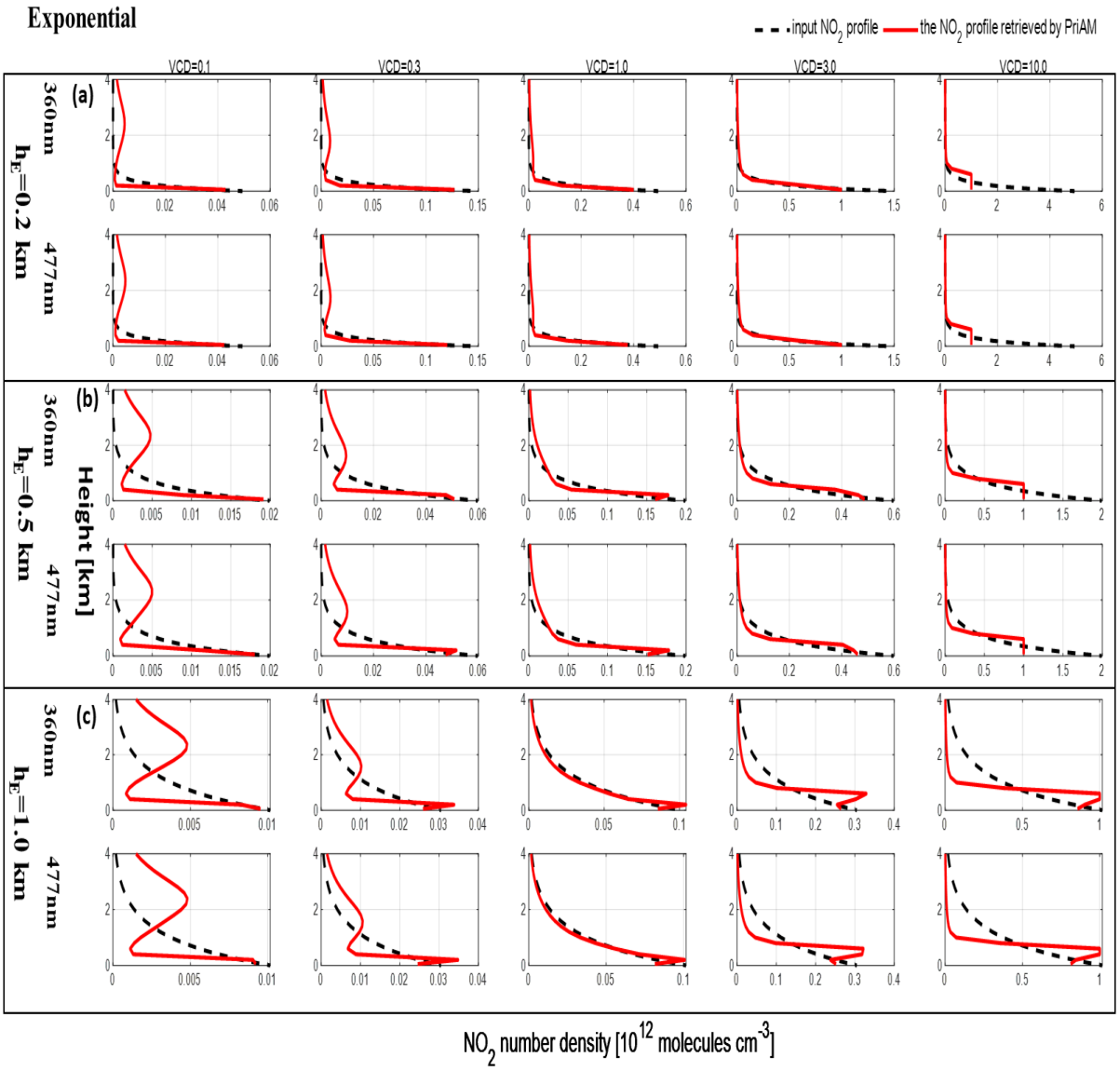

Figure S5. Comparison of NO_2 profiles retrieved by PriAM for 360nm (first line) and 477nm (Second line) with the corresponding input NO_2 profiles for exponential shapes with scale heights of (a) t=0.2km, (b) t=0.5km, and (c) t=1.0km. The AOD was set to 1.0. The black and red curves indicate the input and retrieved NO_2 profiles by PriAM, respectively.

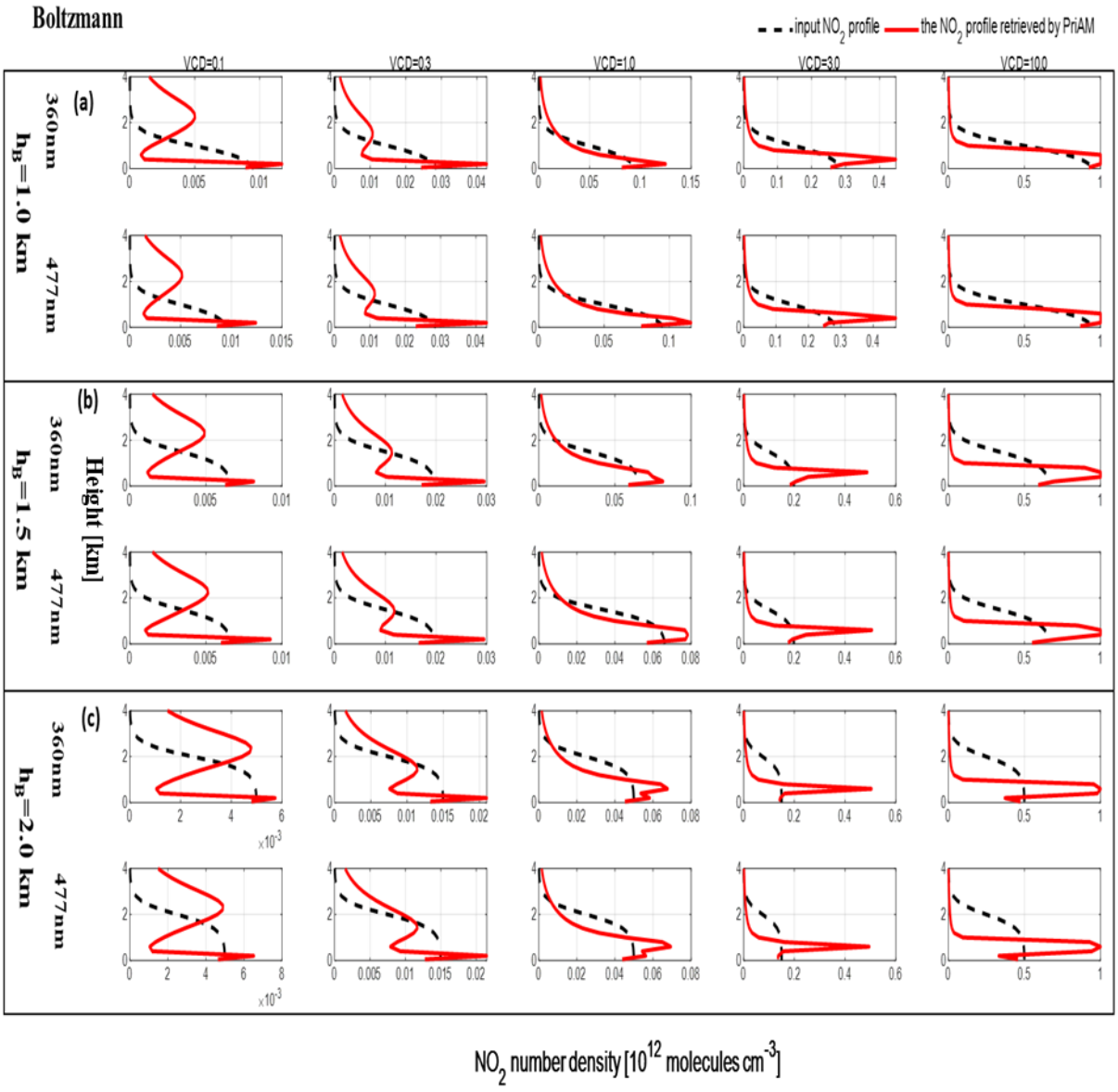

Figure S6. Comparison of NO_2 profiles retrieved by PriAM for 360nm (first line) and 477nm (Second line) with the corresponding input NO_2 profiles for Boltzmann profile shapes with height parameter (a) z=1.0km, (b) z=1.5km, and (c) z=2.0km. The AOD was set to 1.0. The black and red curves indicate the input and retrieved NO_2 profiles by PriAM, respectively.

(I) Gaussian @ h_G= 0.5 km

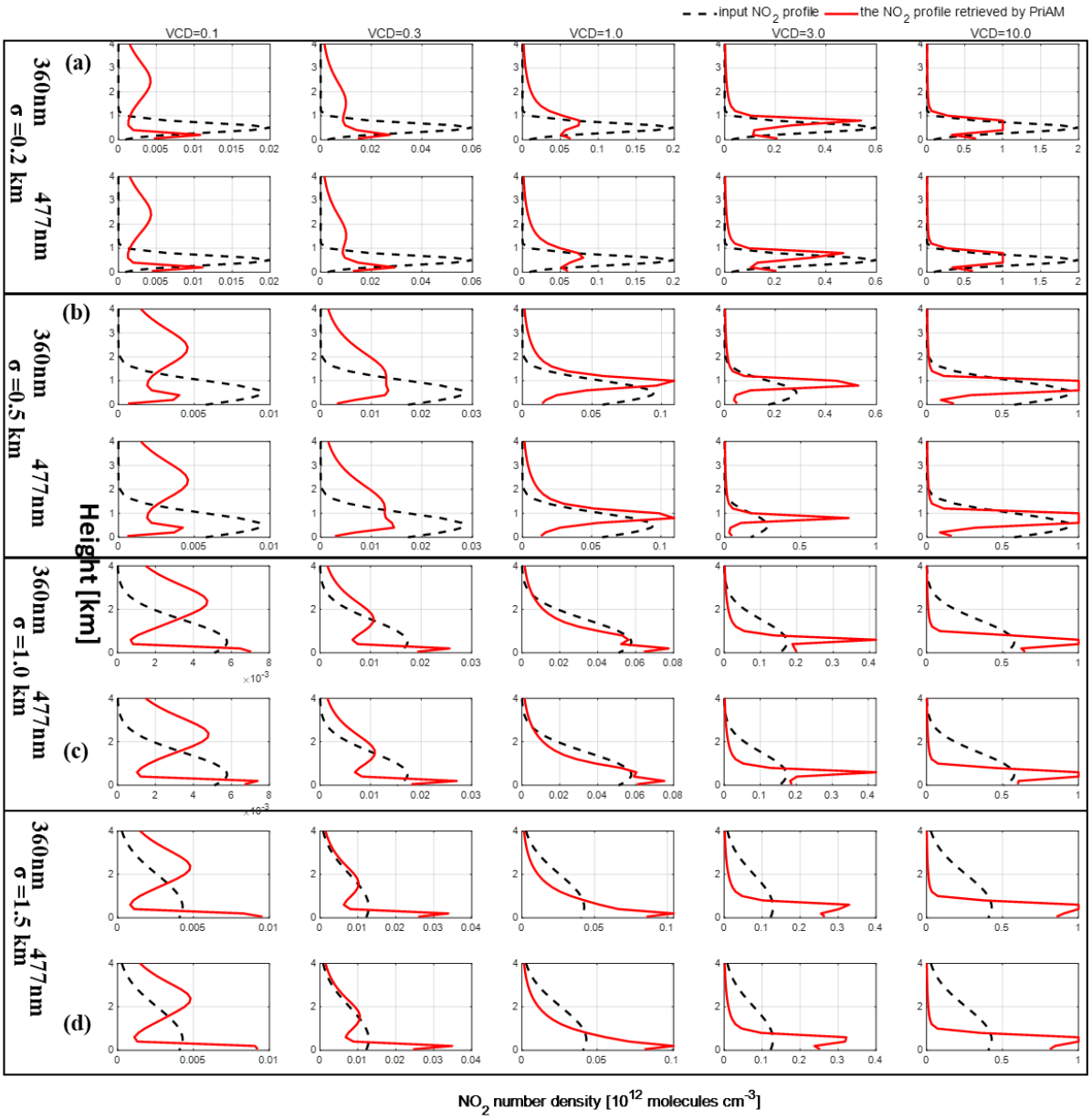

(II) Gaussian @ h_G= 1.0 km

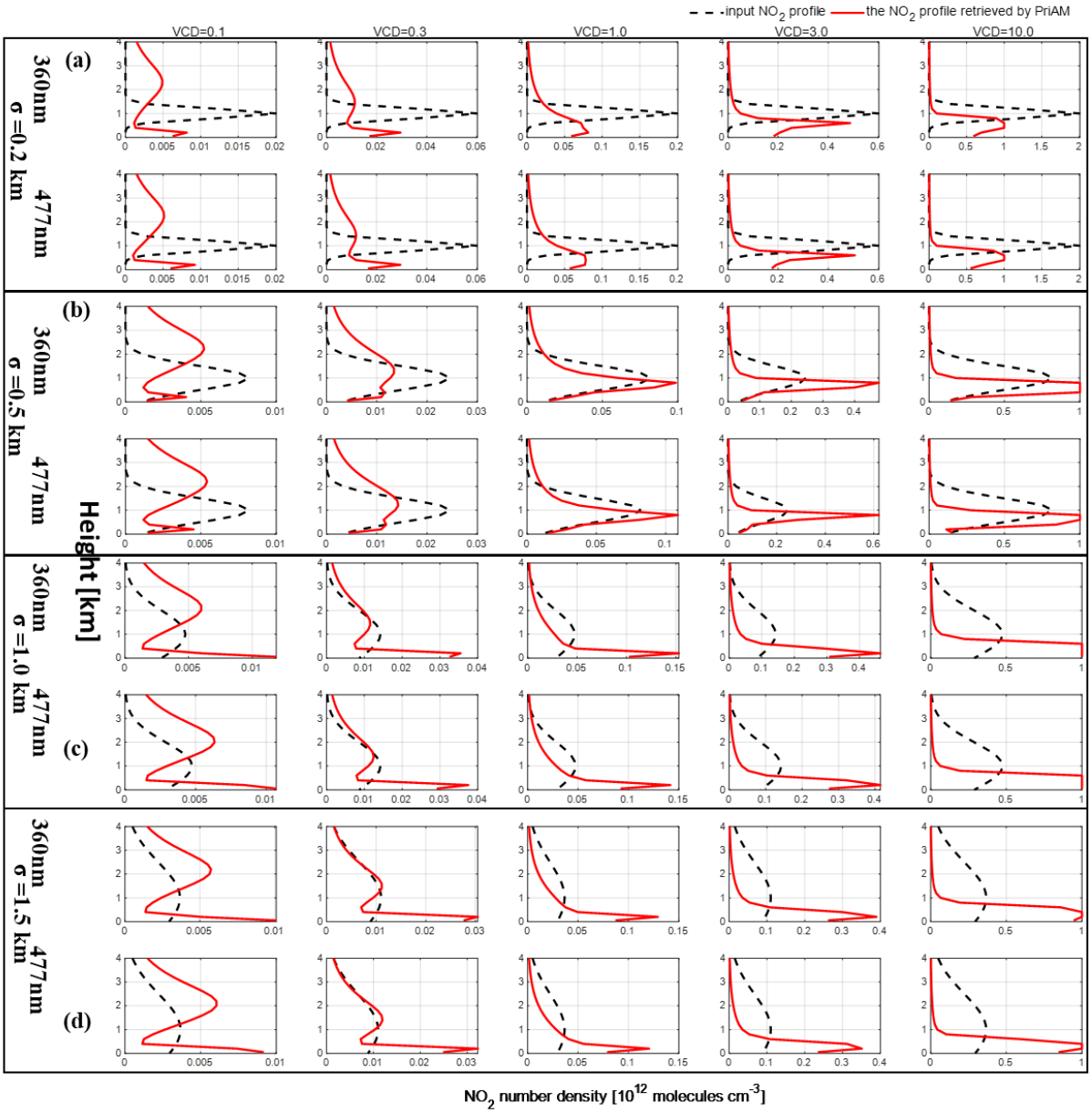

Figure S7. Comparison of NO_2 profiles retrieved by PriAM for 360nm (first line) and 477nm (Second line) with the corresponding input NO_2 profiles for Gaussian shape with different peak heights z_{peak} (I) h_G=0.5km and (II) h_G=1.0km of full width at half maximum (FWHM) σ (a) σ=0.2km, (b) σ=0.5km, (c) σ =1.0km, and (d) σ =1.5km.The AOD was set to 1.0. The black and red curves indicate the input and retrieved NO_2 profiles by PriAM, respectively.

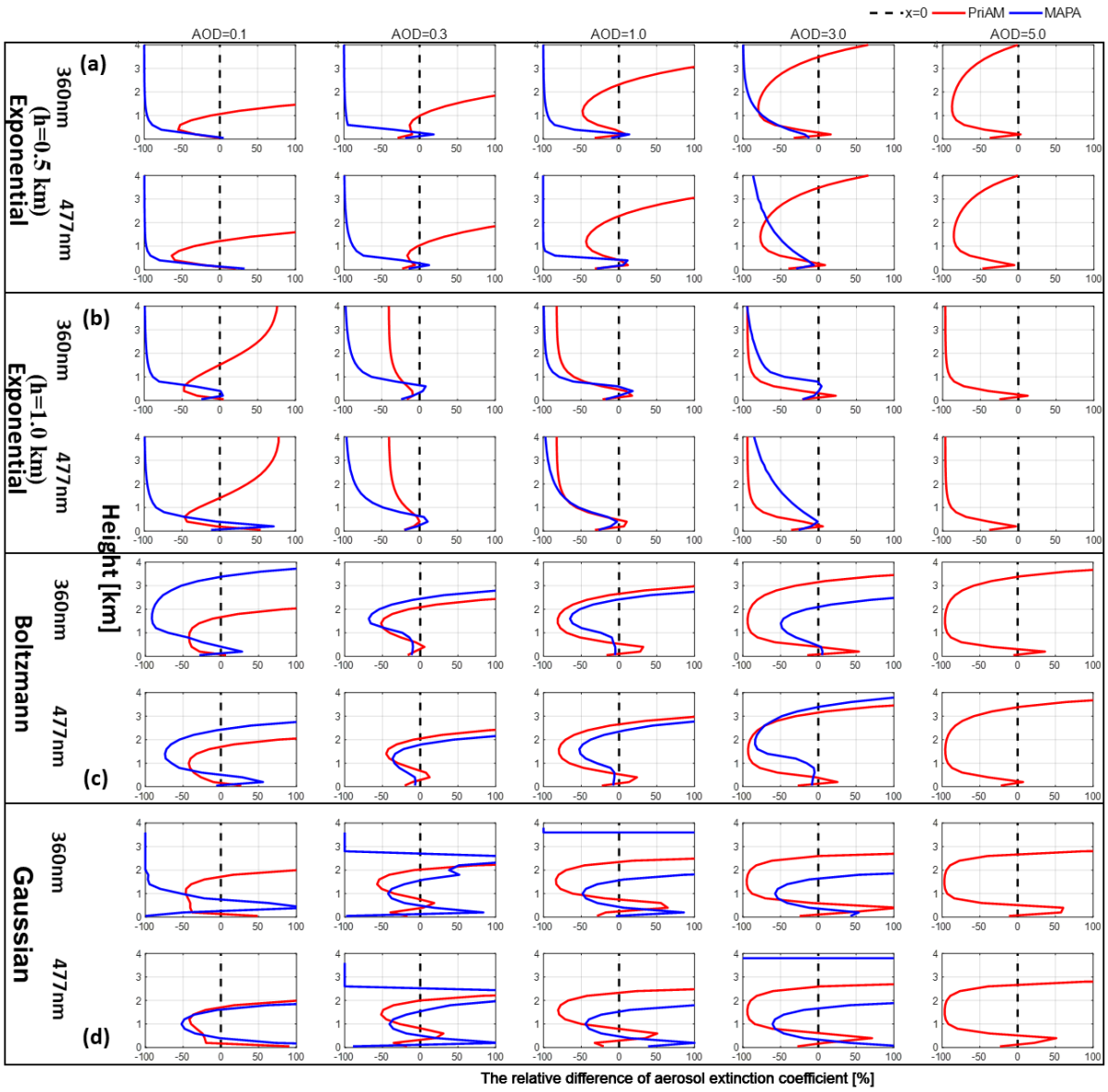

Figure S8. Relative deviations between the profiles retrieved by PriAM and MAPA for 360 nm (first line) and 477 nm (second line) and the corresponding input aerosol profiles for (a) exponential shape with h = 0.5 km, (b) exponential shape with h = 1.0 km, (c) Boltzmann shape, and (d) Gaussian shape.

The red and blue curves indicate the results from PriAM and MAPA, respectively.

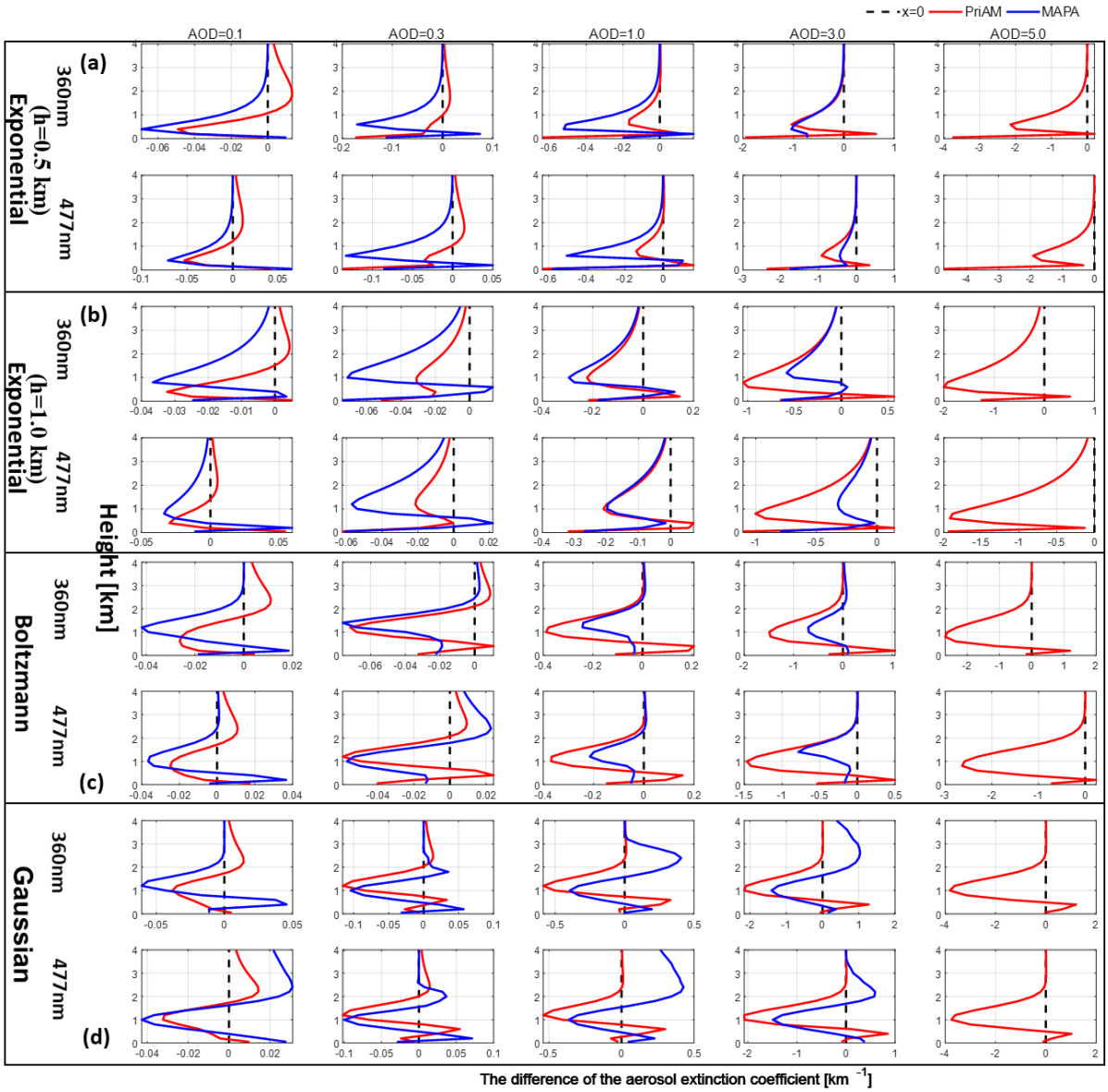

Figure S9. Absolute deviations between the profiles retrieved by PriAM and MAPA for 360 nm (first line) and 477 nm (second line) and the corresponding input aerosol profiles for (a) exponential shape with h = 0.5 km, (b) exponential shape with h = 1.0 km, (c) Boltzmann shape, and (d) Gaussian shape. The red and blue curves indicate the results from PriAM and MAPA, respectively.

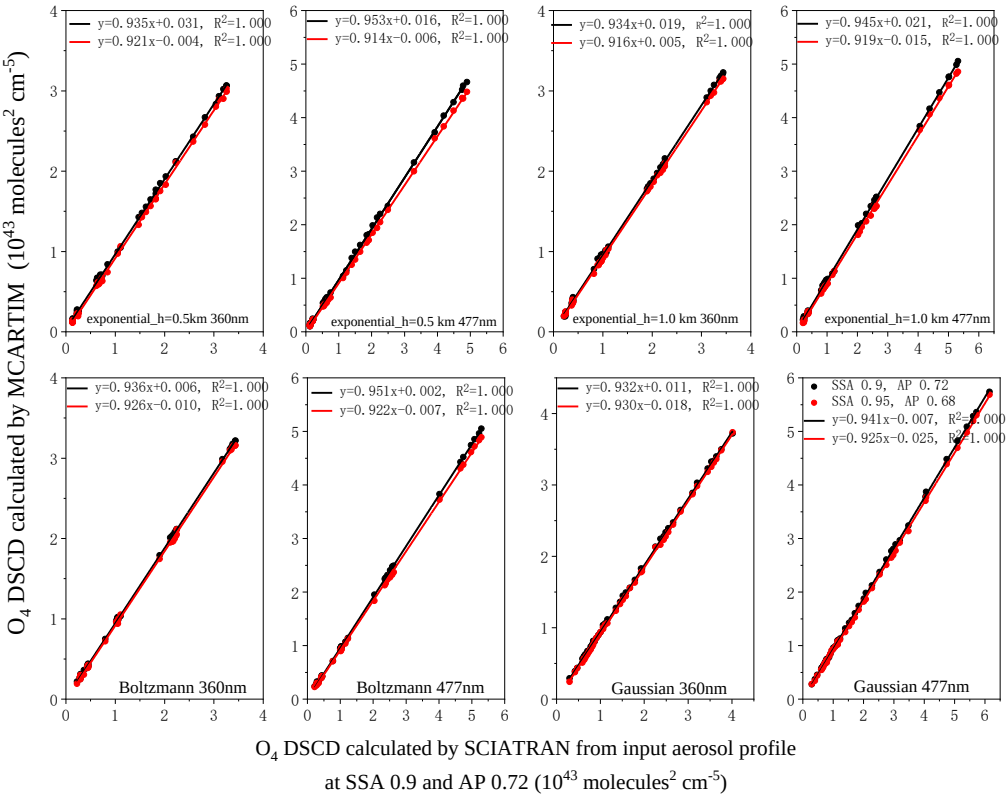

Figure S10. Correlation plots between O_4 DSCDs simulated by MCARTIM for different SSA and AP and SCIATRAN for SSA of 0.90 and AP of 0.72.

The red and black circles indicate the MCARTIM results for SSA=0.95, AP=0.68 and SSA=0.9, AP=0.72, respectively.

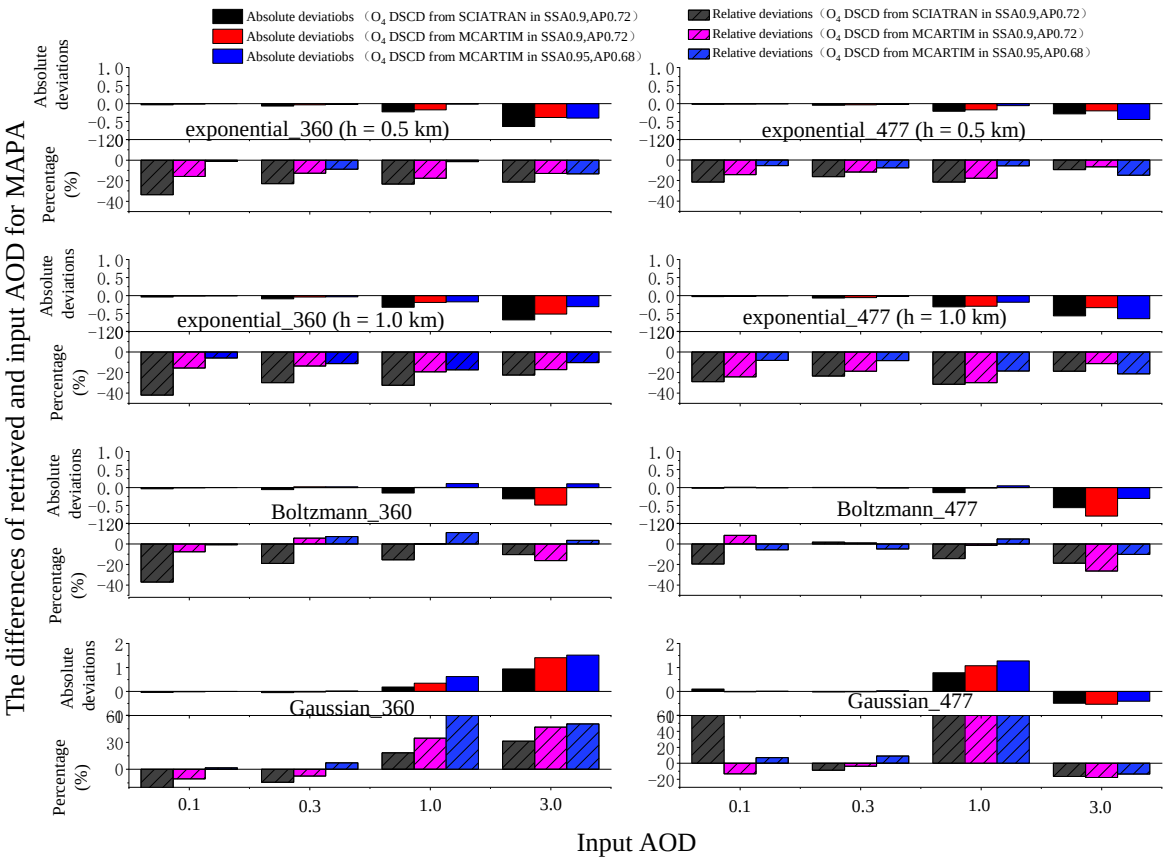

Figure S11. Comparison between the AODs retrieved from MAPA and the input AODs for the 4 aerosol profile shapes listed in table 1. The MAPA AODs were retrieved from the O_4 DSCD simulated by MCARTIM for different SSA and AP and SCIATRAN for SSA of 0.90 and AP of 0.72.

The set of SSA and AP is shown in brackets on top.

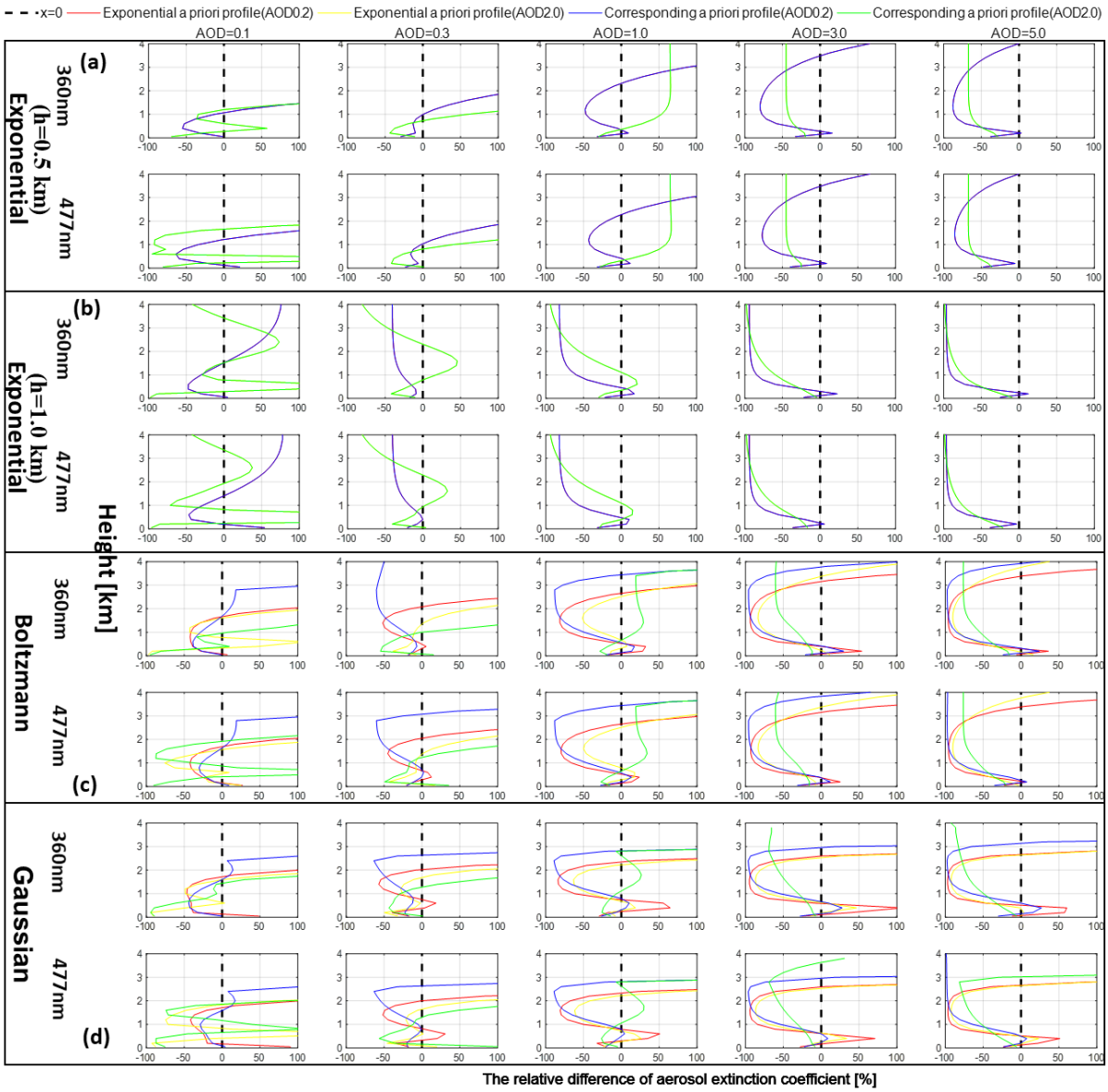

Figure S12. Relative deviations of the PriAM aerosol inversion results with different alternative *a priori* profiles and the results for the universal *a priori* (exponential shape with AOD 0.2).

The first line in every panel denotes the results for 360 nm, and the second line denotes the results for 477 nm. Colors indicate the shapes and AODs shown at the top. 'Corresponding a priori profile' means that the same profile type as the simulated profiles is also used as a priori profile.

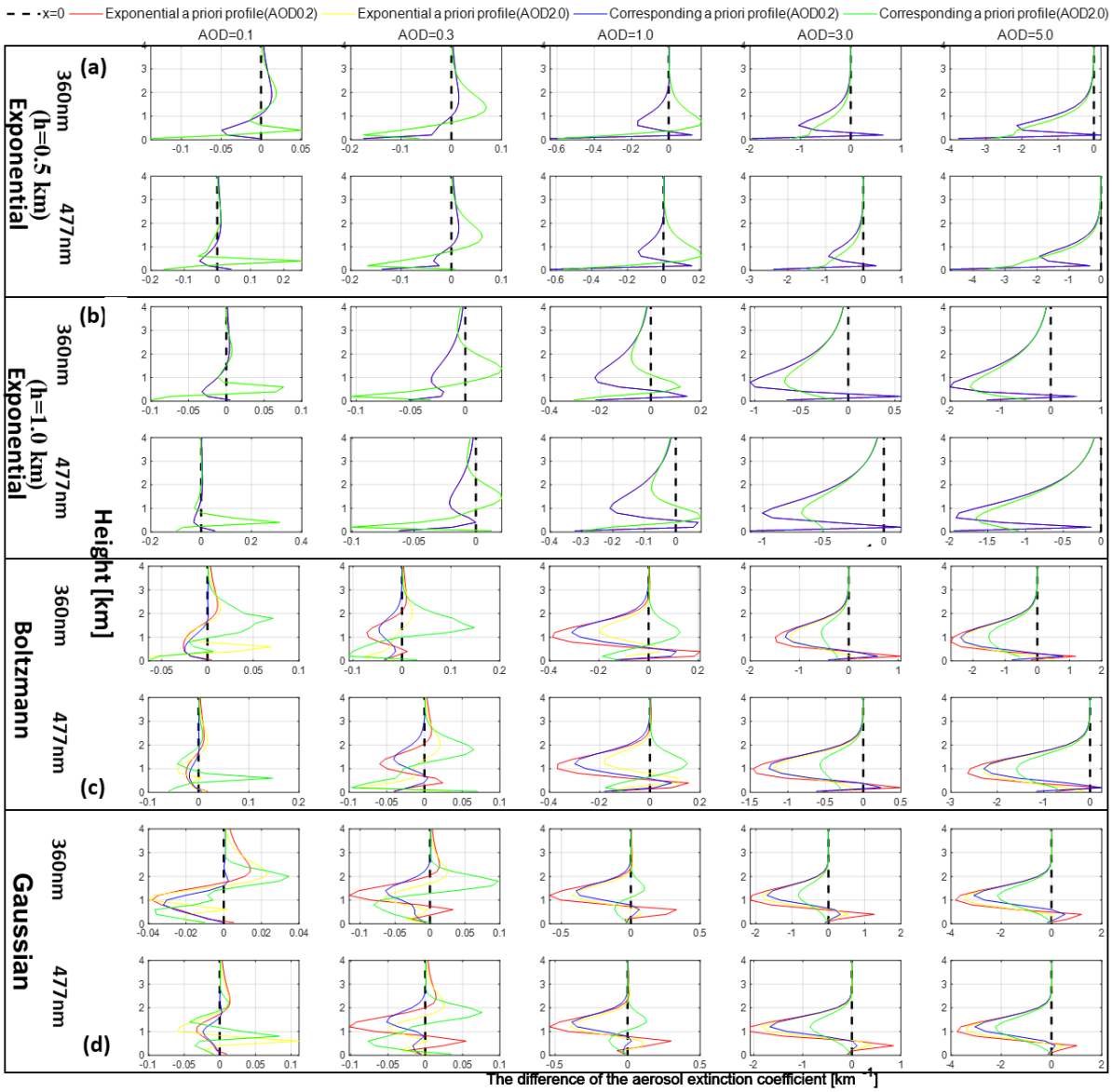

Figure S13. Absolute deviations of the PriAM aerosol inversion results with different alternative *a priori* profiles and the results for the universal *a priori* (exponential shape with AOD 0.2). The first line in every panel denotes the results for 360 nm, and the second line denotes the results for 477 nm. Colors indicate the shapes and AODs shown at the top. 'Corresponding a priori profile' means that the same profile type as the simulated profiles is also used as a priori profile.

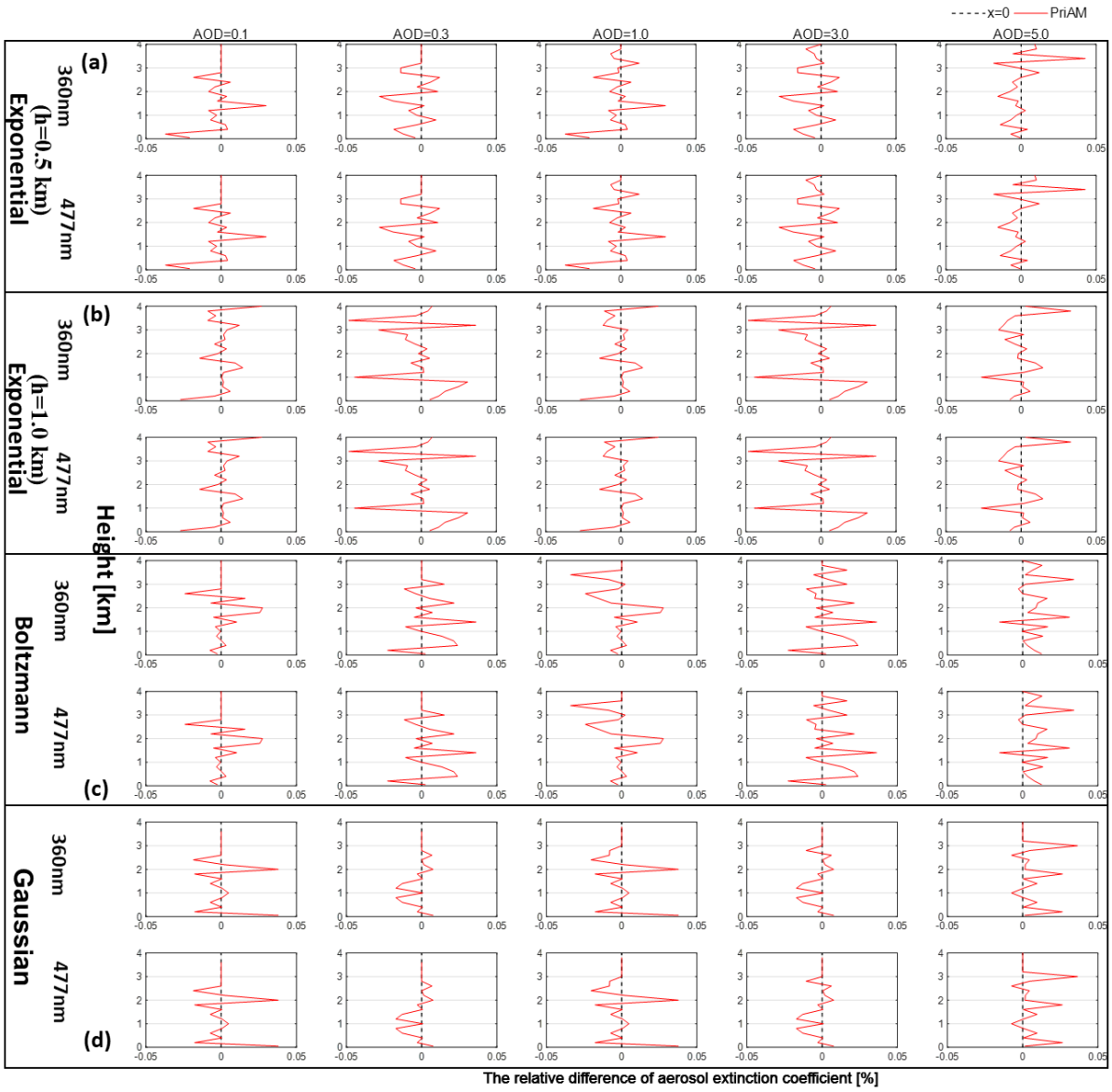

Figure S14. Relative deviations of the input aerosol profile and the PriAM inversion results if the exact a priori profiles are used as input profiles.

The first line in every panel denotes the results for 360 nm, and the second line denotes the results for 477 nm. The black and red curves indicate the input (the same as the *a priori* profile) and retrieved aerosol profiles by PriAM, respectively.

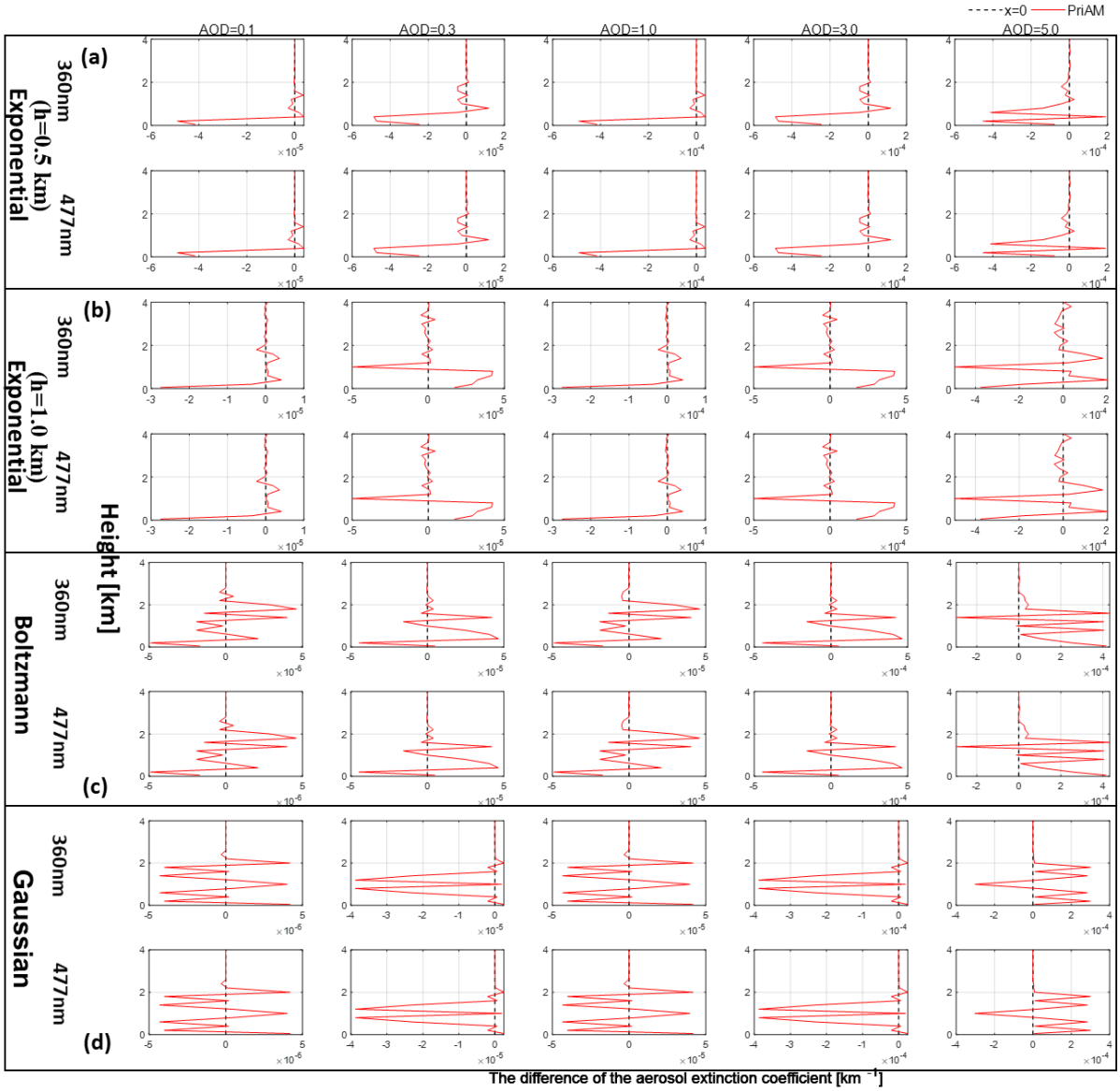

Figure S15. Absolute deviations of the input aerosol profile and the PriAM inversion results if the exact a priori profiles are used as input profiles.

The first line in every panel denotes the results for 360 nm, and the second line denotes the results for 477 nm. The black and red curves indicate the input (the same as the *a priori* profile) and retrieved aerosol profiles by PriAM, respectively.

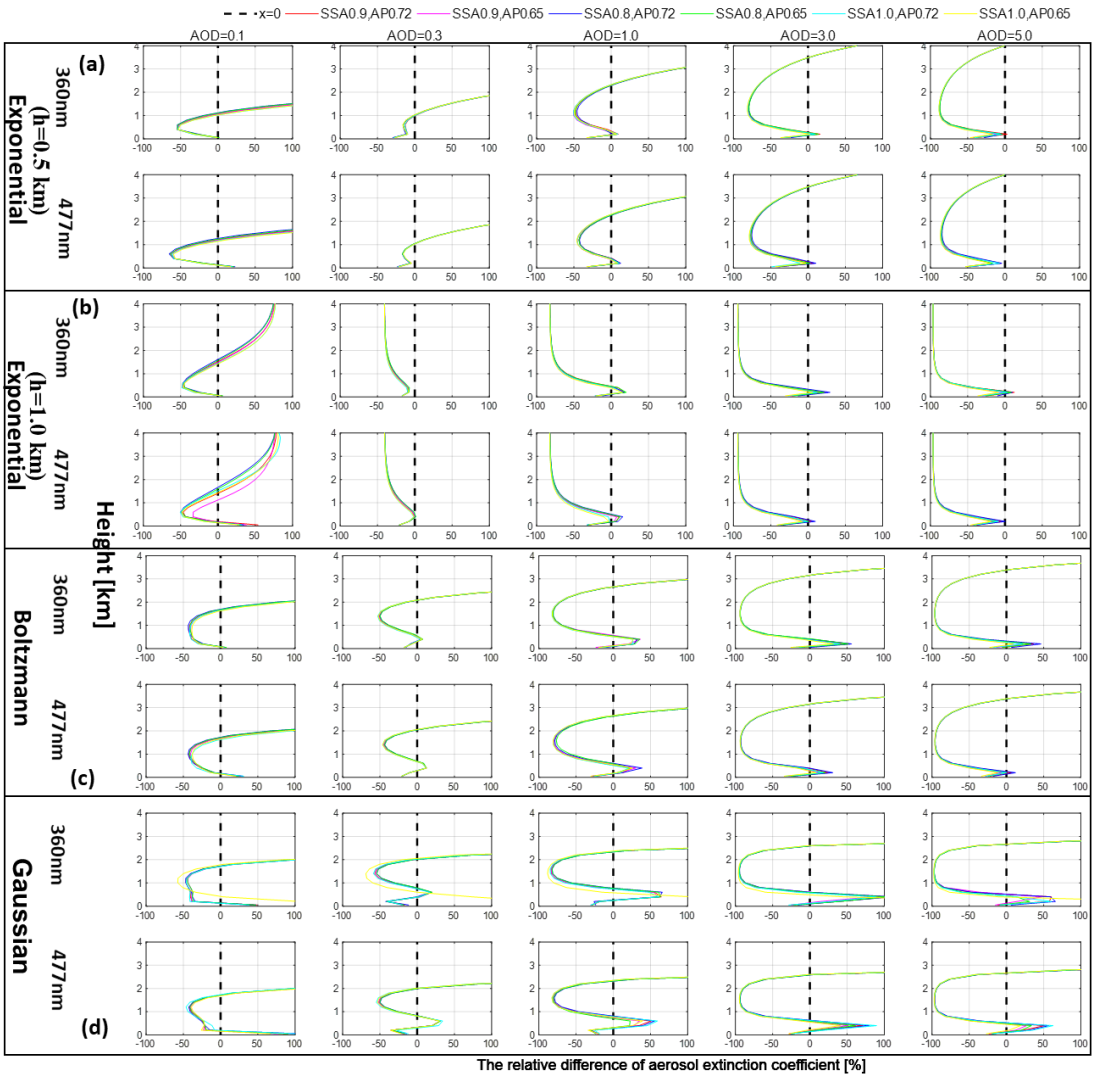

Figure S16. Relative deviations between the PriAM results using different SSA and AP and the input aerosol profile results for (a) exponential shape with h = 0.5 km, (b) exponential shape with h = 1.0 km, (c) Boltzmann shape, and (d) Gaussian shape. For these inversions, the same SSA and AP were used for the simulations of the O_4 DSCDs and for the PriAM inversions. The first line in every panel denotes the results for 360 nm, and the second line denotes the results for 477 nm. The colors refer to the corresponding SSA and AP values shown at the top.

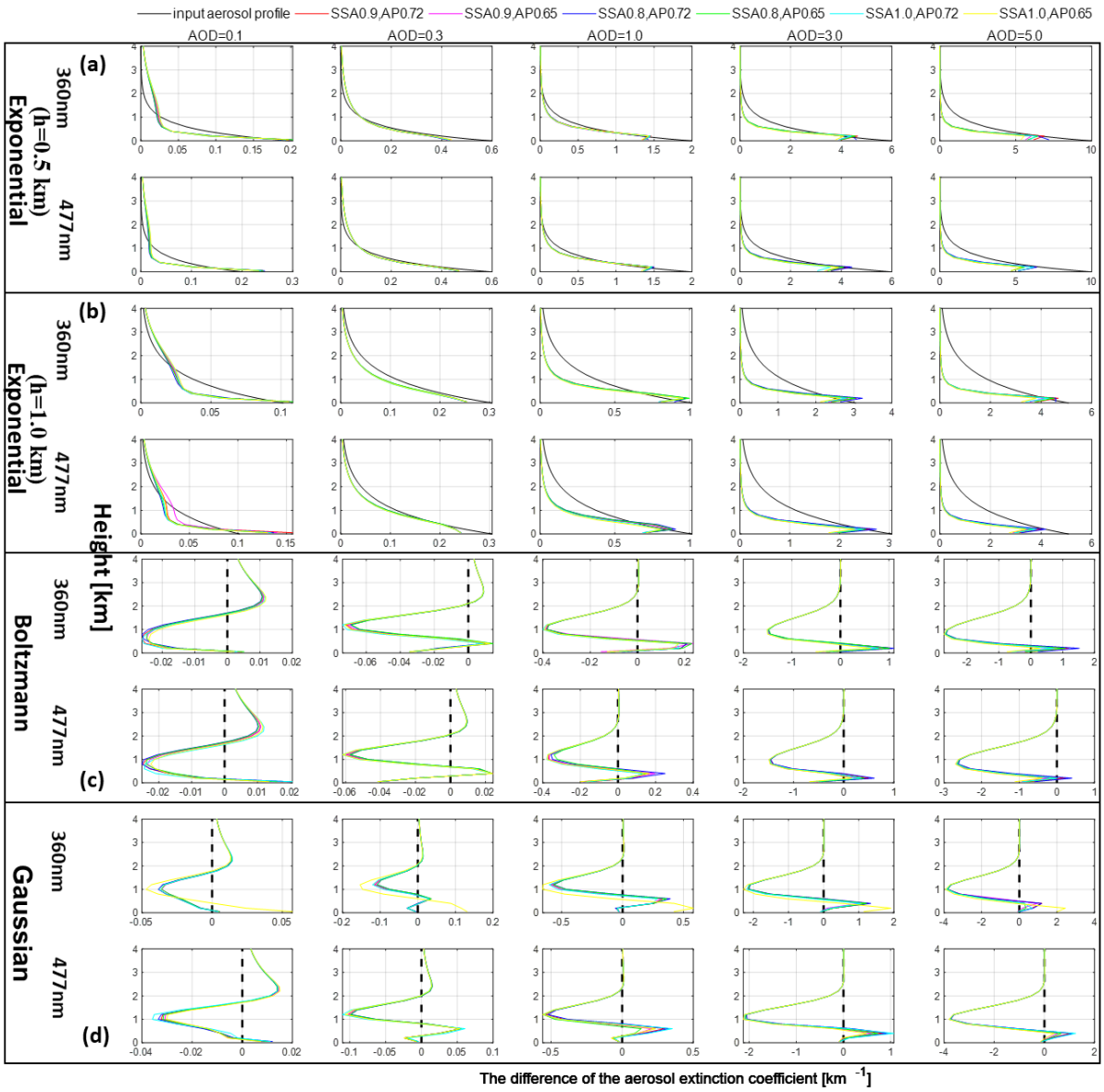

Figure S17. Absolute deviations between the PriAM results using different SSA and AP and the input aerosol profile results of (a) exponential shape with h = 0.5 km, (b) exponential shape with h= 1.0 km, (c) Boltzmann shape, and (d) Gaussian shape. For these inversions, the same SSA and AP values were used for the simulations of the O_4 DSCDs and for the PriAM inversions. The first line in every panel denotes the results for 360 nm, and the second line denotes the results for 477 nm.

The colors refer to the corresponding SSA and AP shown at the top.

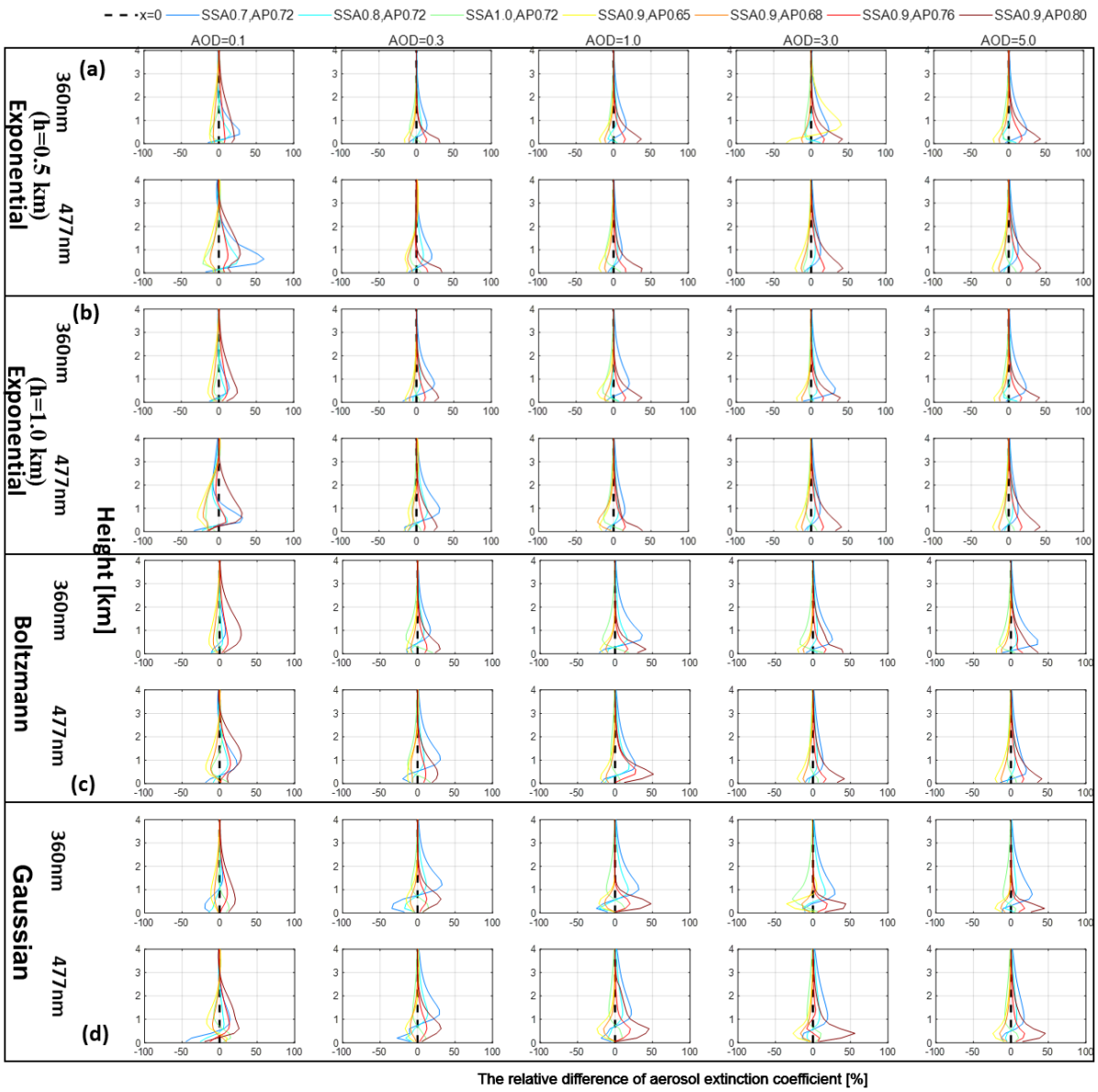

Figure S18. Relative deviations of the retrieved profiles using incorrect SSA and AP values from the retrieved profiles with the correct SSA and AP values for (a) exponential shape with h = 0.5 km, (b) exponential shape with h = 1.0 km, (c) Boltzmann shape, and (d) Gaussian shape

The colors refer to the SSA and AP values shown at the top.

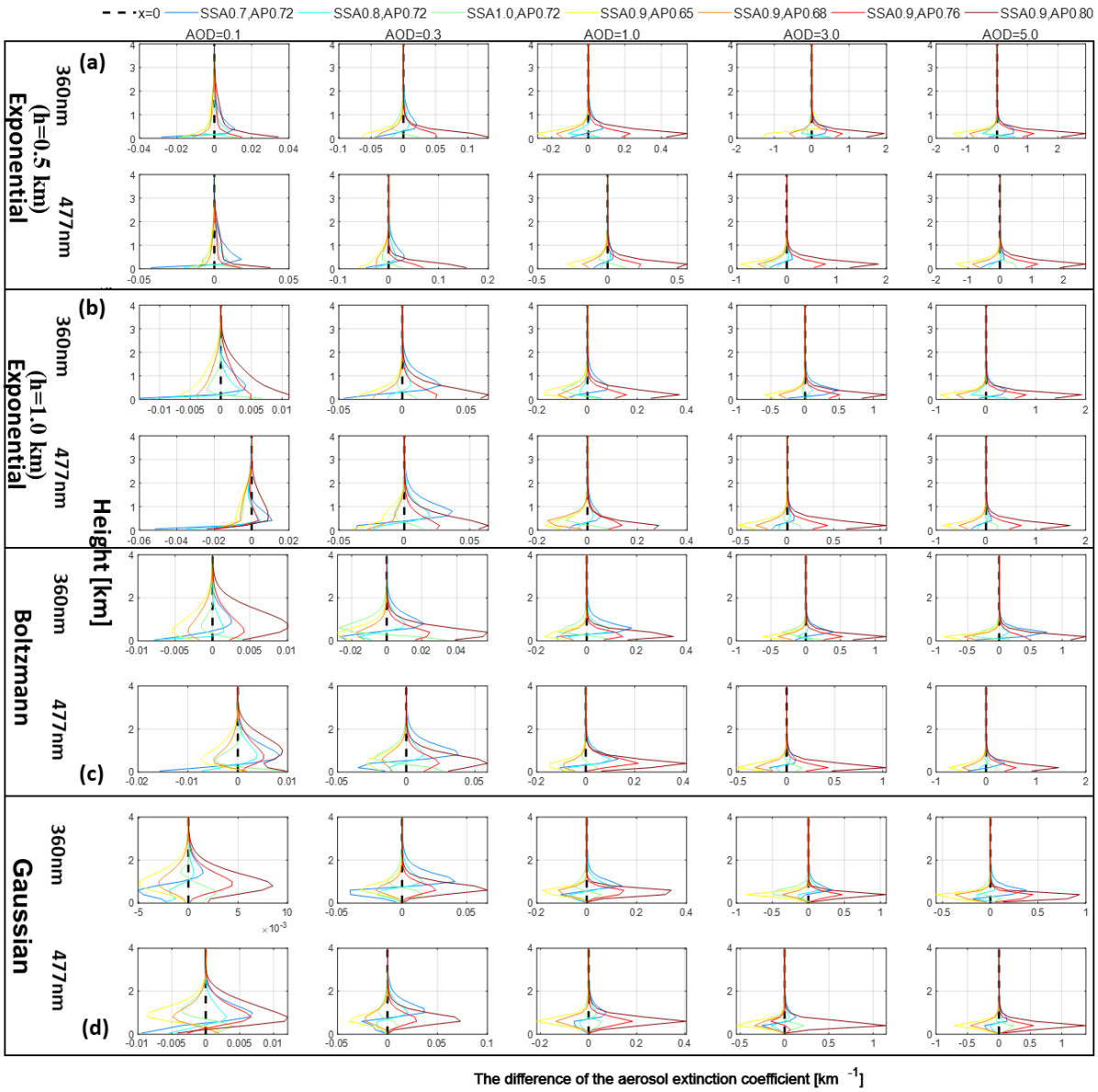

Figure S19. Absolute deviations of the retrieved aerosol profiles using incorrect SSA and AP values from the profiles retrieved with the correct SSA and AP values for (a) exponential shape with h = 0.5 km, (b) exponential shape with h = 1.0 km, (c) Boltzmann shape, and (d) Gaussian shape.

The colors refer to the SSA and AP values shown at the top.

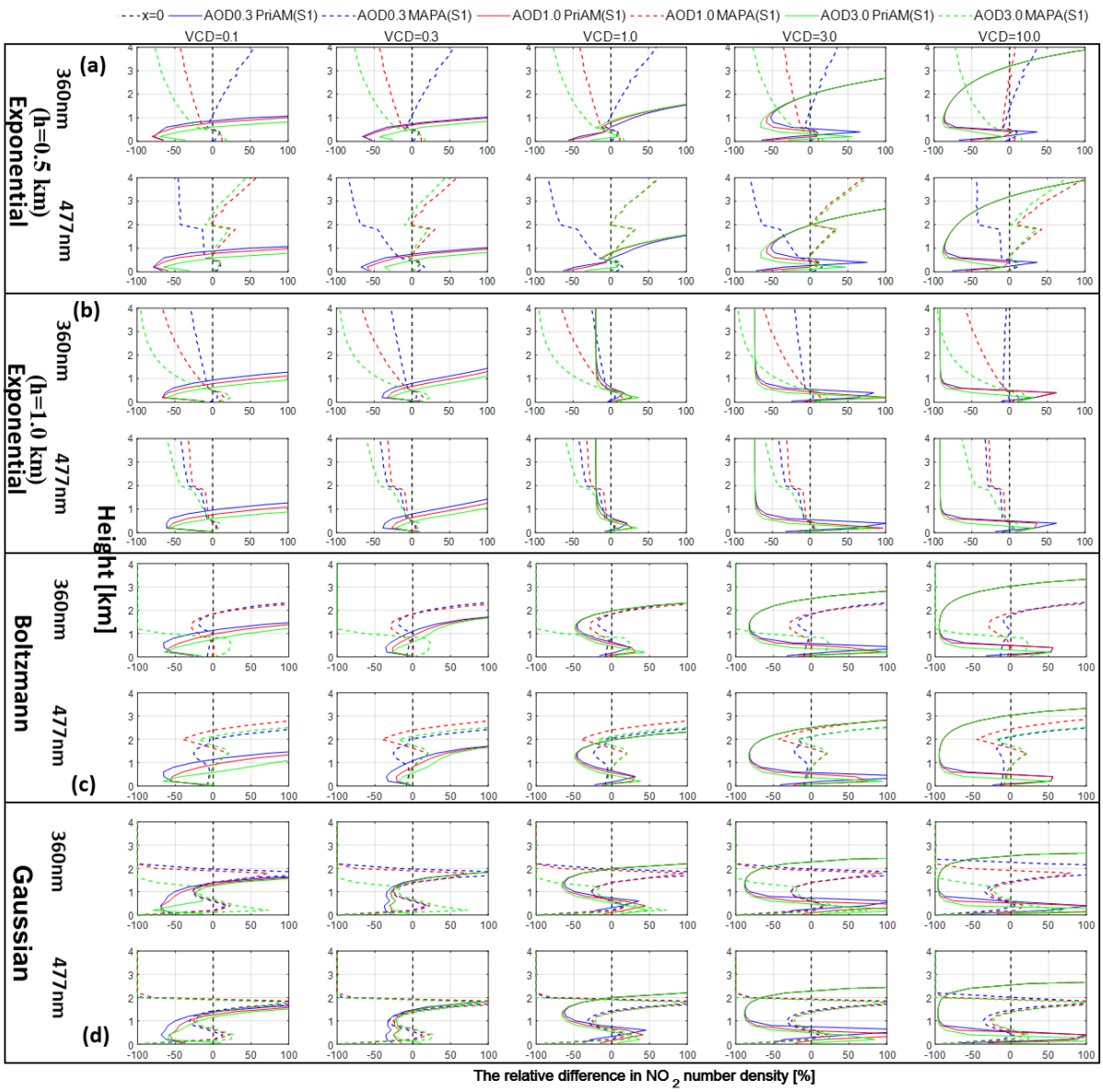

Figure S20. Relative deviations of the retrieved NO_2 profiles by PriAM and MAPA from the input NO_2 profiles for scenario S1 (see text) for aerosol profiles with 3 selected AODs (0.3, 1.0, and 3.0) and 5 NO_2 VCDs for of (a) exponential shape with h = 0.5 km, (b) exponential shape with h = 1.0 km, (c) Boltzmann shape, and (d) Gaussian shape.

The solid and dotted colored lines refer to the AODs and algorithms shown at the top.

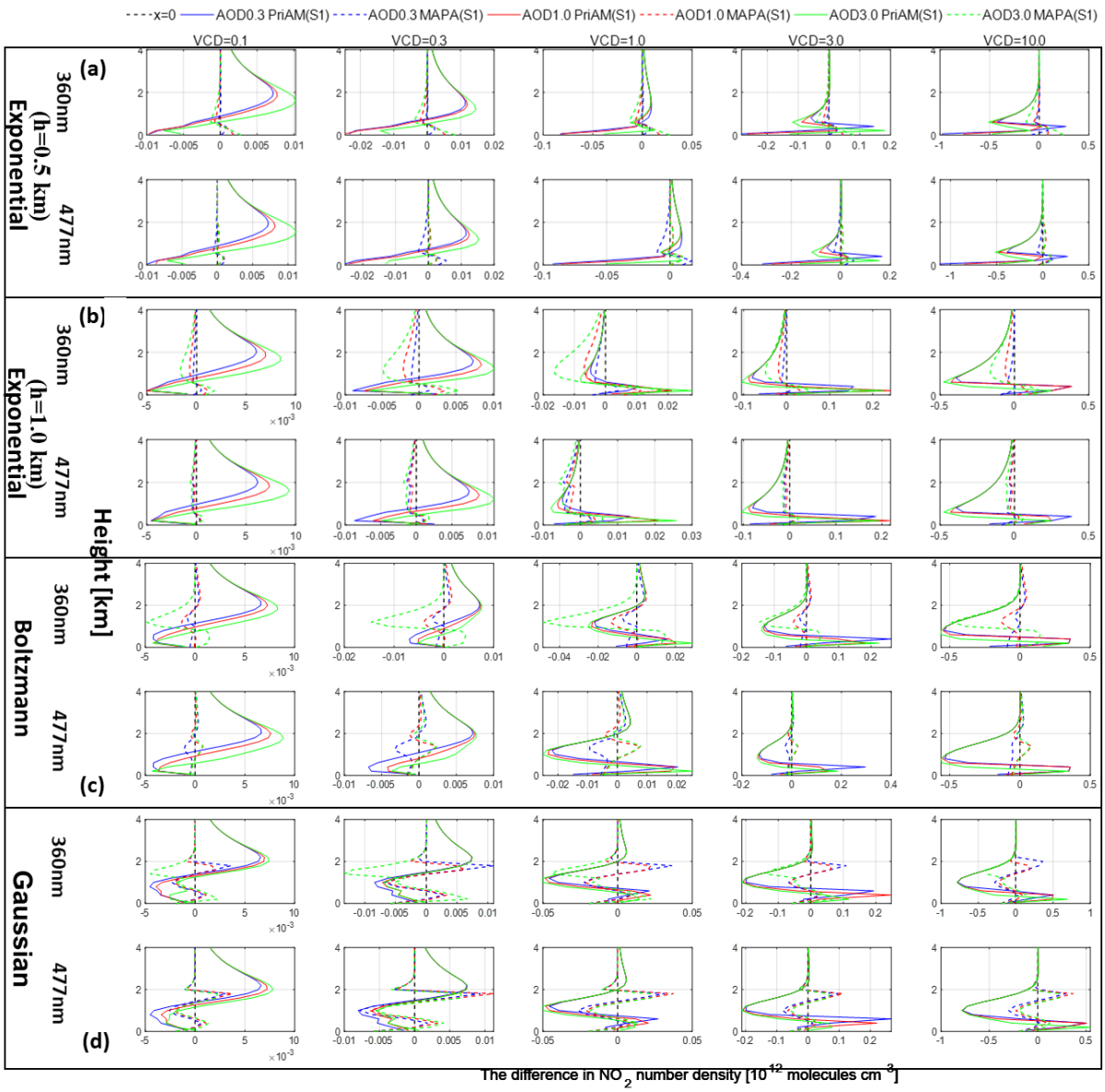

Figure S21. Absolute deviation of the retrieved NO_2 profiles by PriAM and MAPA from the input NO_2 profiles for scenario S1 (see text) for aerosol profiles with 3 selected AODs (0.3, 1.0, and 3.0) and 5 NO_2 VCDs for of (a) exponential shape with h= 0.5 km, (b) exponential shape with h = 1.0 km, (c) Boltzmann shape, and (d) Gaussian shape.

The solid and dotted colored lines refer to the AODs and algorithms shown at the top.

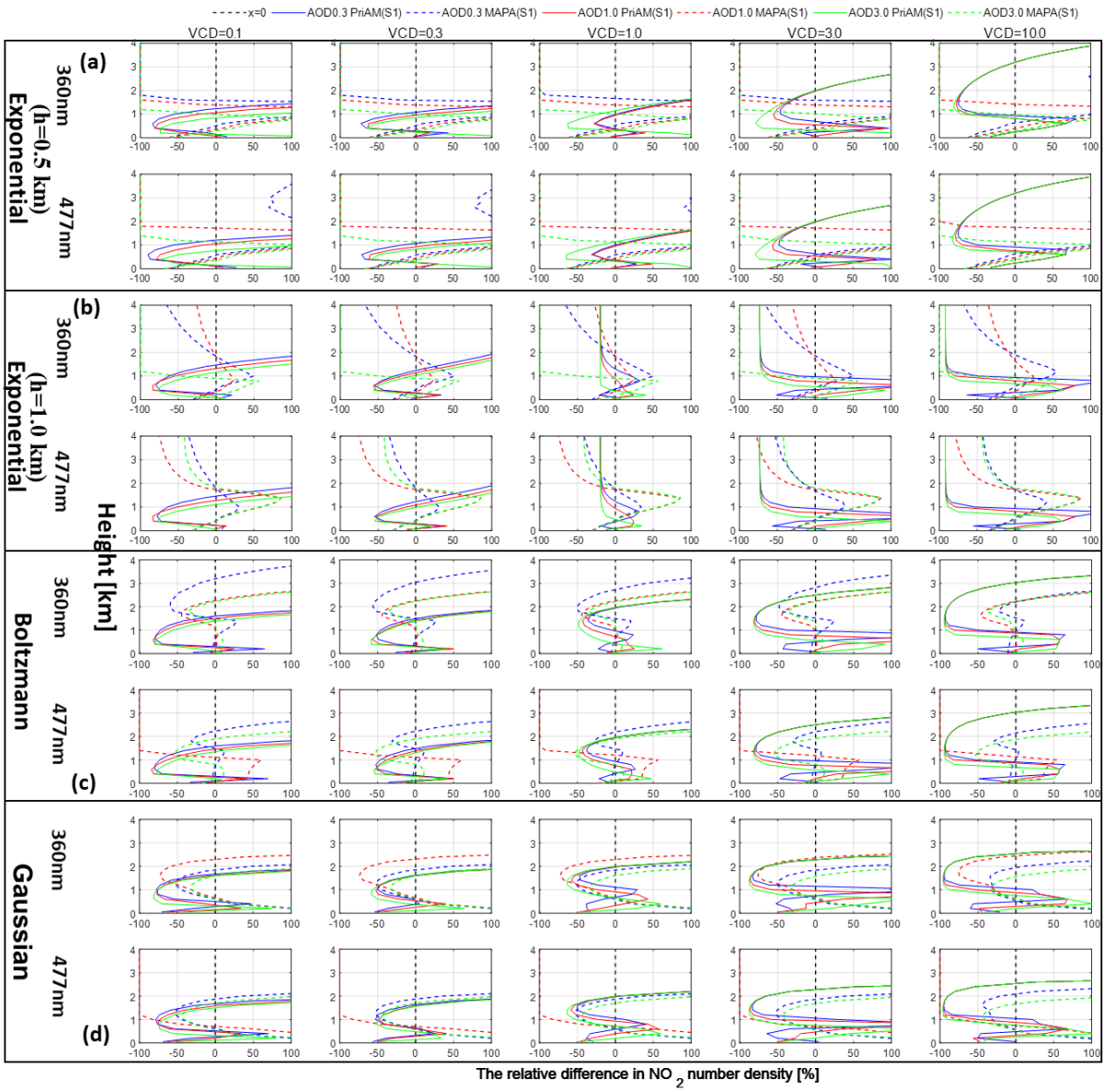

Figure S22. Relative deviations of the retrieved NO_2 profiles for Boltzmann NO_2 input profiles by PriAM and MAPA from the input NO_2 profiles for scenario S1 (see text) and for 4 aerosol profile shapes ((a) exponential shape with h = 0.5 km, (b) exponential shape with h = 1.0 km, (c) Boltzmann shape, and (d) Gaussian shape) with 3 selected AODs (0.3, 1.0, and 3.0) and 5 NO_2 VCDs.

The solid and dotted colored lines refer to the AODs and algorithms shown at the top.

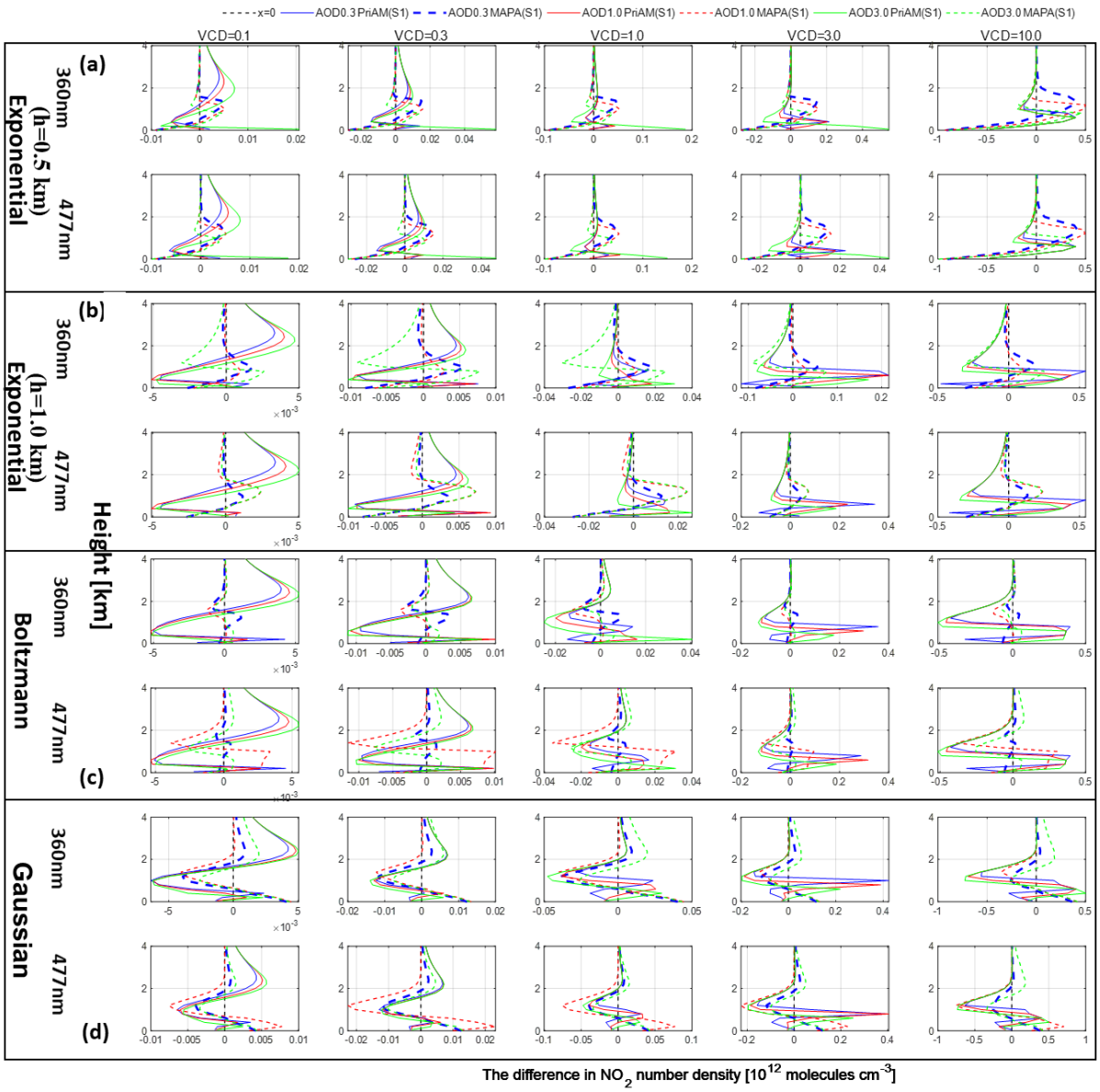

Figure S23. Absolute deviations of the retrieved NO_2 profiles for Boltzmann NO_2 input profiles by PriAM and MAPA from the input NO_2 profiles for scenario S1 (see text) and for 3 aerosol profile shapes ((a) exponential shape with h = 0.5 km, (b) exponential shape with h = 1.0 km, (c) Boltzmann shape, and (d) Gaussian shape) with 3 selected AODs (0.3, 1.0, and 3.0) and 5 NO2 VCDs. The solid and dotted colored lines refer to the AODs and algorithms shown at the top.

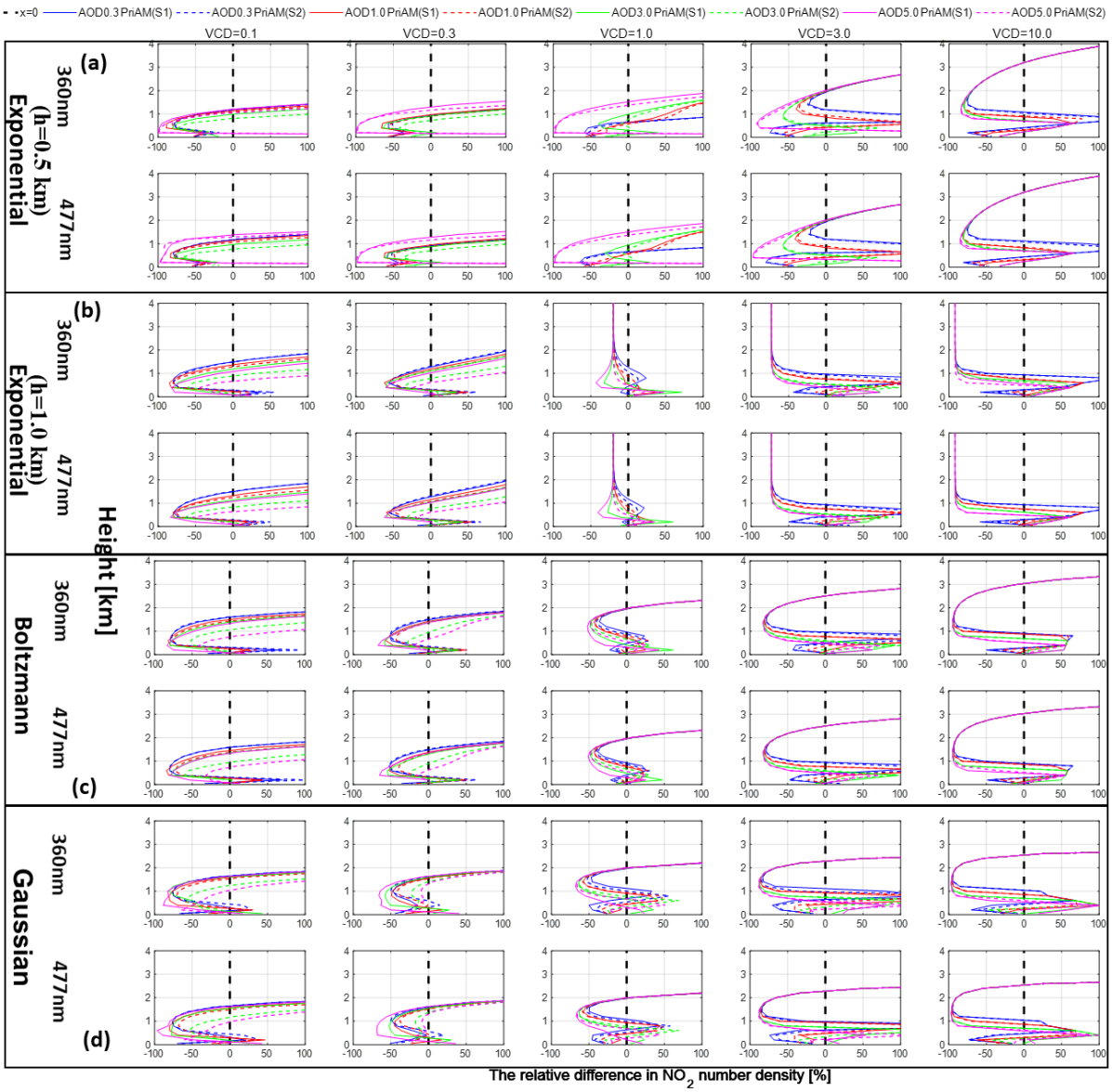

Figure S24. Relative deviations between the NO_2 profiles retrieved by PriAM for scenarios S1 and S2 and the input NO_2 profiles for 4 AODs (0.3, 1.0, 3.0, and 5.0) and 5 VCDs and for the (a) exponential shape with h = 0.5 km, (b) exponential shape with h= 1.0 km, (c) Boltzmann shape, and (d) Gaussian shape.

The first line in each panel denotes the results for 360 nm, and the second line denotes the results for 477 nm. The solid and dotted colored lines refer to the AODs and strategies shown at the top.

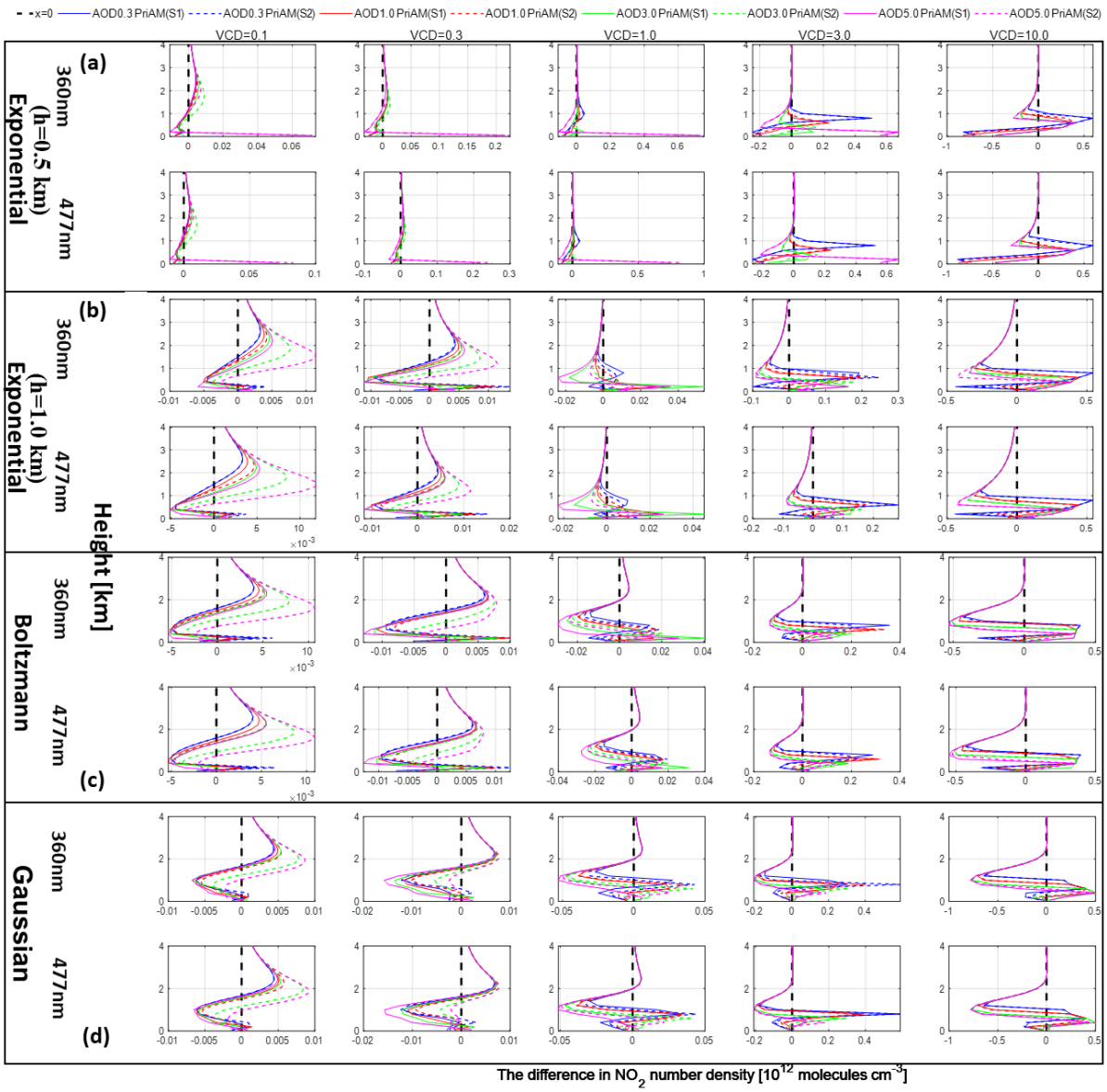

Figure S25. Absolute deviations between the NO_2 profiles retrieved by PriAM for scenarios S1 and S2 and the input NO_2 profiles for 4 AODs (0.3, 1.0, 3.0, and 5.0) and 5 VCDs and for (a) exponential shape with h = 0.5 km, (b) exponential shape with h = 1.0 km, (c) Boltzmann shape, and (d) Gaussian shape.

The first line in each panel denotes the results for 360 nm, and the second line denotes the results for 477 nm. The solid and dotted colored lines refer to the AODs and strategies shown at the top.

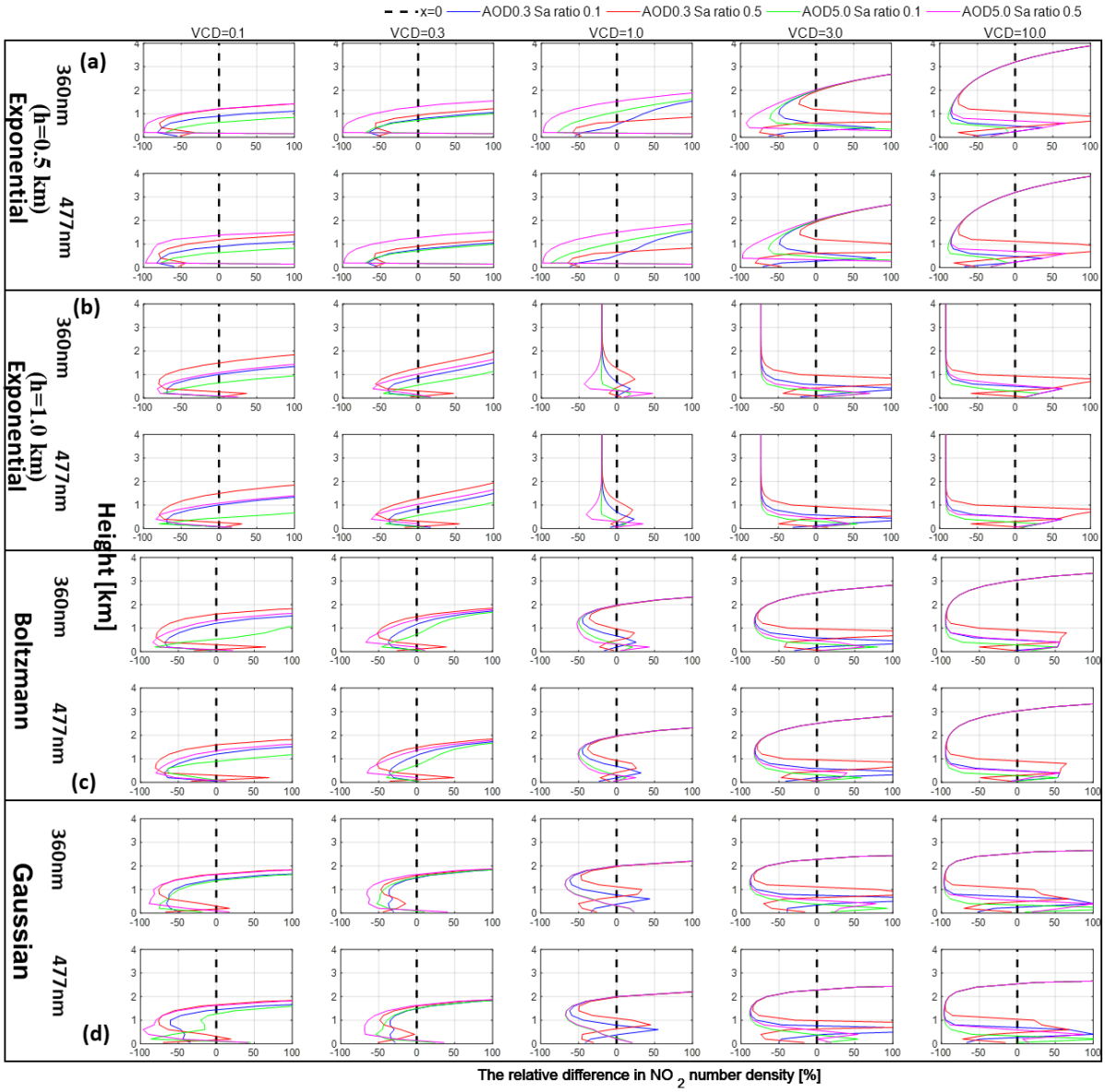

Figure S26. Relative deviations for NO_2 profiles retrieved by PriAM and the input NO_2 profiles for Sa of 0.1 and 0.5 and AOD of 0.3 and 5.0 and for (a) exponential shape with h = 0.5 km, (b) exponential shape with h = 1.0 km, (c) Boltzmann shape, and (d) Gaussian shape.

The first line in each panel denotes the results for 360 nm, and the second line denotes the results for 477 nm. The solid and dotted colored lines refer to the AODs and Sa_ratio shown at the top.

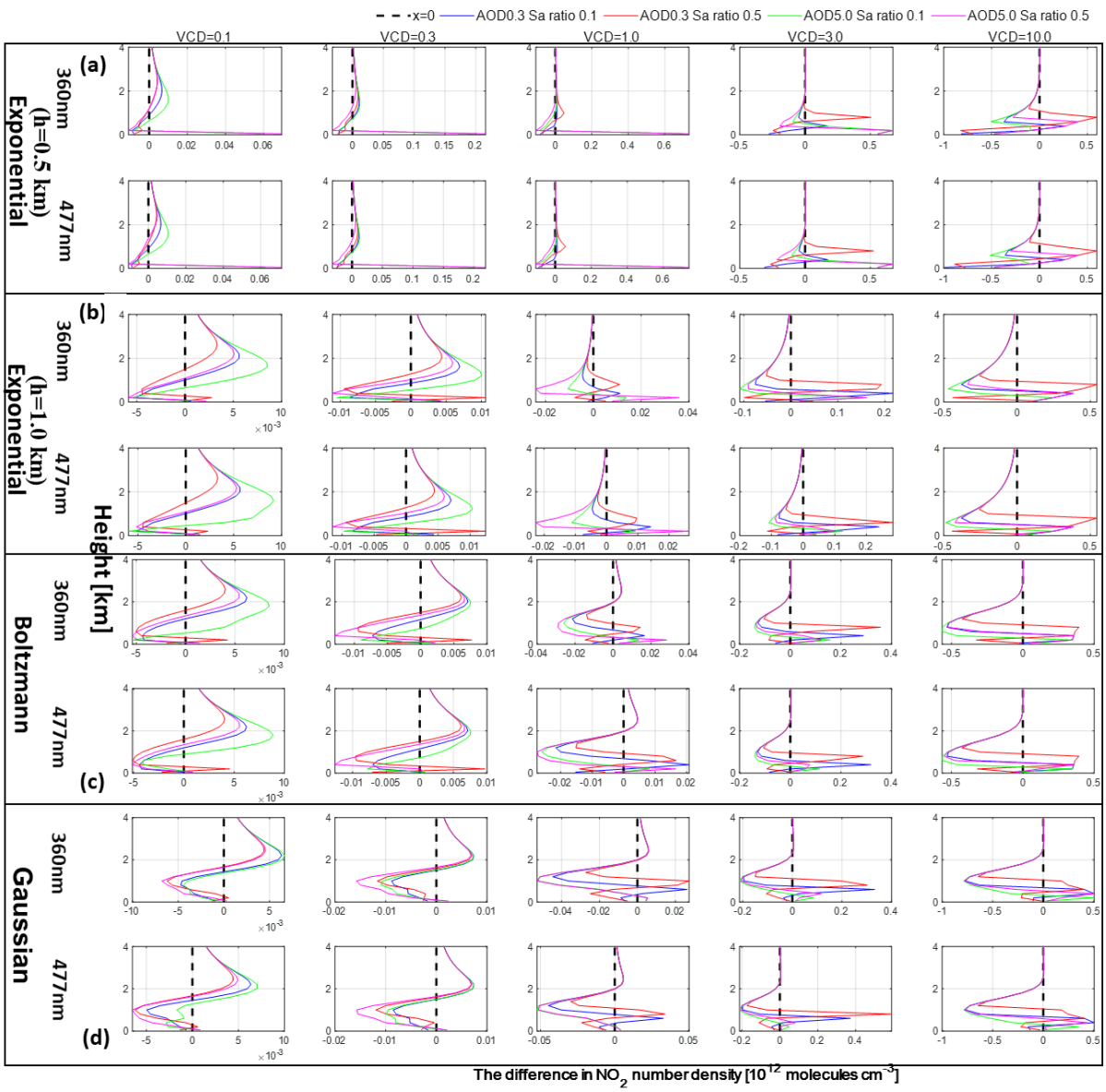

Figure S27. Absolute deviations between NO_2 profiles retrieved by PriAM and the input NO_2 profiles for Sa of 0.1 and 0.5 and AOD of 0.3 and 5.0s for (a) exponential shape with h = 0.5 km, (b) exponential shape with h = 1.0 km, (c) Boltzmann shape, and (d) Gaussian shape.

The first line in each panel denotes the results for 360 nm, and the second line denotes the results for 477 nm. The solid and dotted colored lines refer to the AODs and Sa_ratio shown at the top.

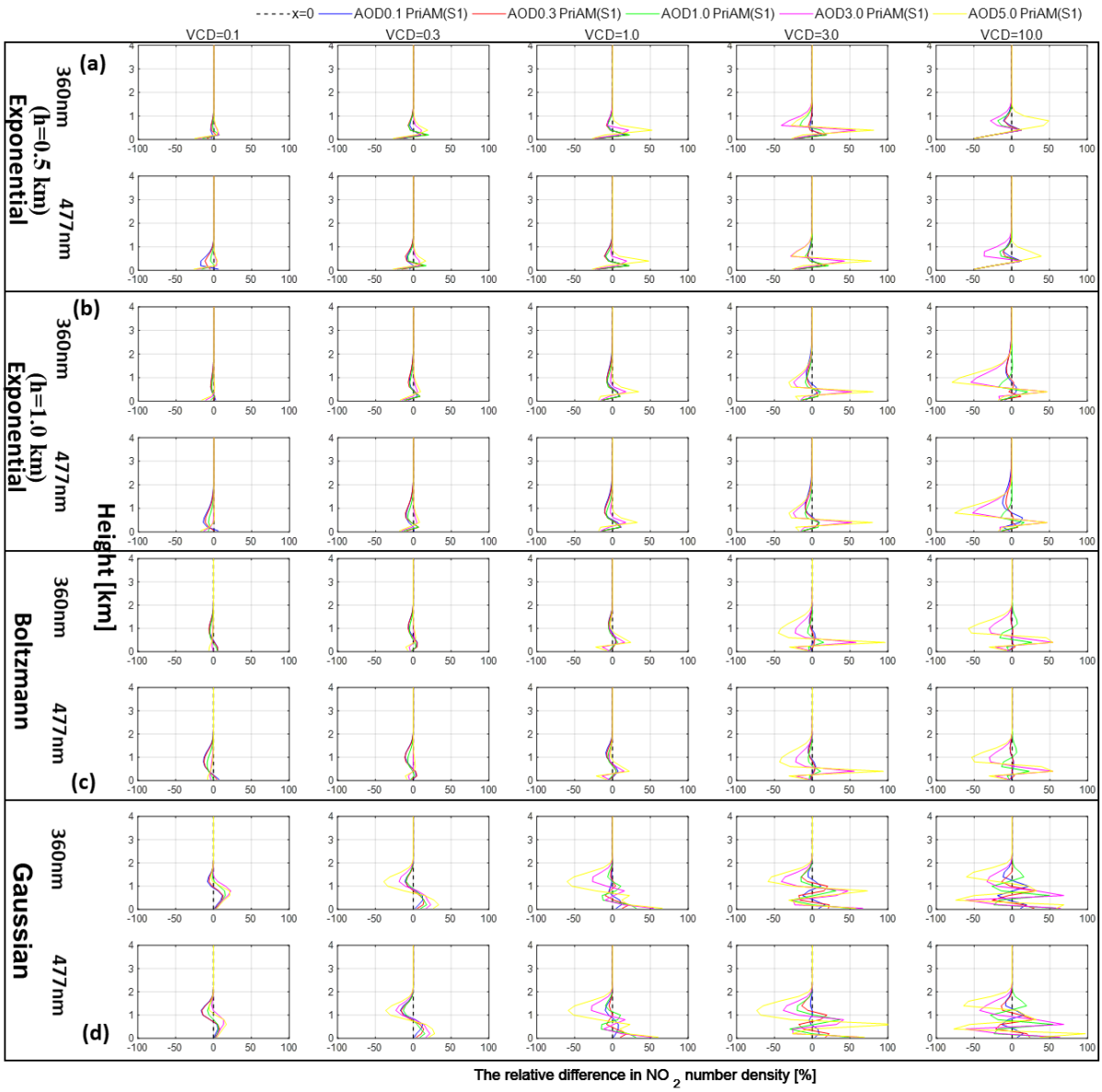

Figure S28. Relative deviations between the input NO_2 profiles and NO_2 profiles retrieved by PriAM if exactly the a priori profiles for aerosols and NO_2 are used as input profiles for 5 AODs (0.1, 0.3, 1.0, 3.0, and 5.0) and 5 NO_2 VCDs for of (a) exponential shape with h = 0.5 km, (b) exponential shape with h = 1.0 km, (c) Boltzmann shape, and (d) Gaussian shape.

The solid colored lines refer to the AODs and algorithms shown at the top

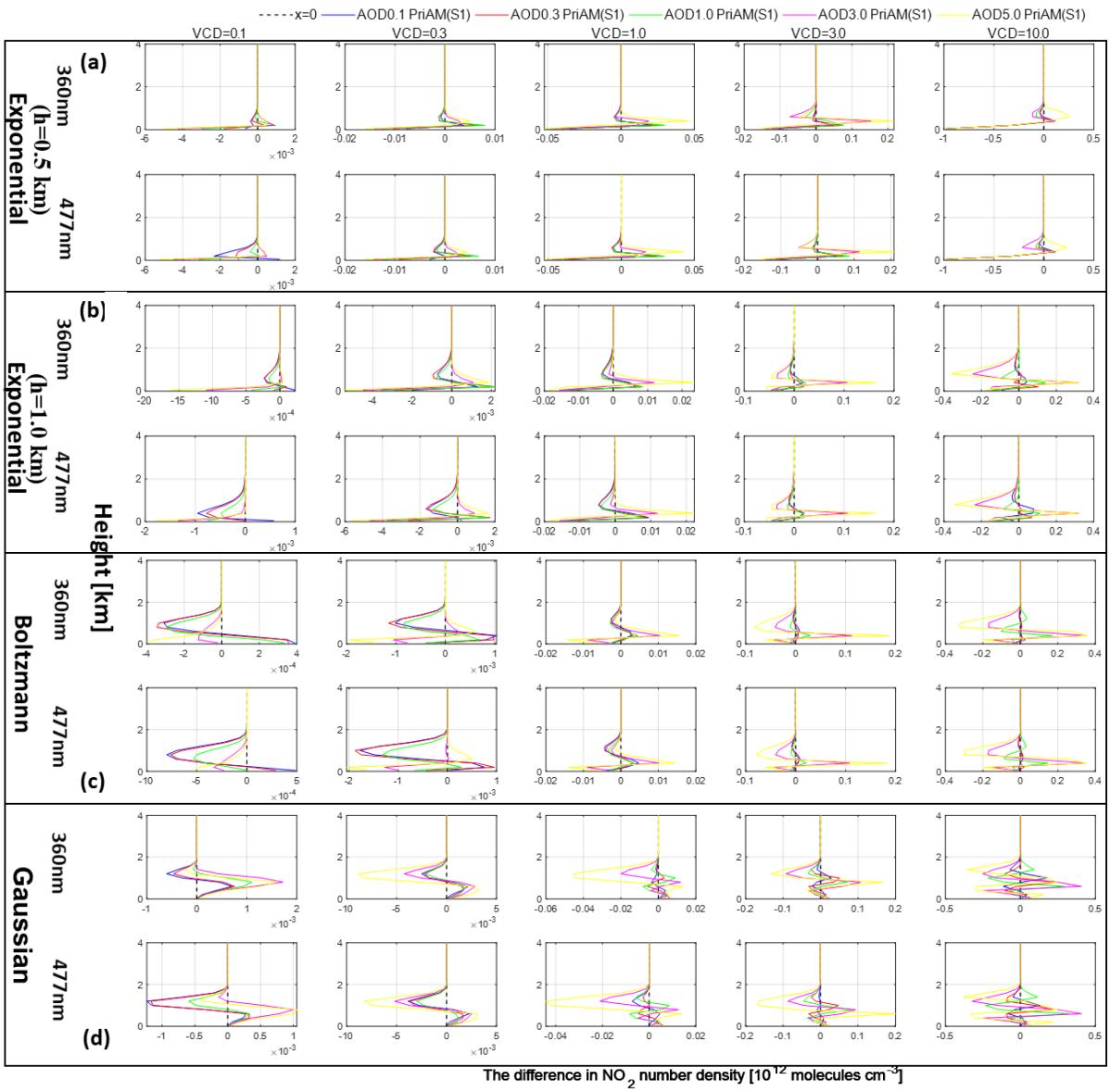

Figure S29. Absolute deviations between the input NO_2 profiles and NO_2 profiles retrieved by PriAM if exactly the a priori profiles for aerosols and NO_2 are used as input profiles for 5 AODs (0.1, 0.3, 1.0, 3.0, and 5.0) and 5 NO_2 VCDs for of (a) exponential shape with h = 0.5 km, (b) exponential shape with h = 1.0 km, (c) Boltzmann shape, and (d) Gaussian shape.

The solid colored lines refer to the AODs and algorithms shown at the top